POTENTIAL ROLE OF ATP8A1 AS PLASMA MEMBRANE AMINOPHOSPHOLIPID TRANSLOCASE IN PROLIFERATING NEURONAL CELLS

by

Kelly Levano

A dissertation submitted to the Graduate Faculty in Biochemistry in partial fulfillment of the requirements for the degree of

Doctor of Philosophy

The City University of New York

2009

This manuscript has been read and accepted by the Graduate Faculty in Biochemistry in satisfaction of the dissertation requirements for the degree of Doctor of Philosophy

_____	_____
Date	Chairperson of Examining Committee
	Dr. Probal Banerjee
_____	_____
Date	Executive Officer
	Dr. Edward J. Kennelly

_____

Dr. Jimmie Fata, The College of Staten Island, CUNY

_____

Dr. Mitchell Goldfarb, Hunter College, CUNY

_____

Dr. Yu-Wen Hwang, NY State Institute for Basic Research

_____

Dr. Chang-Hui Shen, The College of Staten Island, CUNY

Supervisory Committee

THE CITY UNIVERSITY OF NEW YORK

THE CITY UNIVERSITY OF NEW YORK

ABSTRACT

POTENTIAL ROLE OF ATP8A1 AS PLASMA MEMBRANE AMINOPHOSPHOLIPID TRANSLOCASE IN PROLIFERATING NEURONAL CELLS

by

Kelly Levano

Advisor: Professor Probal Banerjee

The inner leaflet-localized phospholipid PS undergoes a translocation to the outer leaflet of the plasma membrane in apoptotic cells to trigger recognition and phagocytic removal of these dying cells by PS receptor-bearing scavenger cells, such as microglia and macrophages. The enzyme activity responsible for the inner-membrane localization of PS is the plasma membrane aminophospholipid translocase (PLAPLT), also known as flippase, which translocates PS from the outer to the inner leaflet of the plasma membrane. Attempts to identify the PLAPLT molecule of mammalian cells have revealed a candidate molecule, Atp8a1, which is a P-type Mg-ATPase. After much controversy, it is currently believed that Atp8a1 translocates PS across internal membranes but not the plasma membrane. Based on our earlier studies showing overexpression of Atp8a1 in proliferating hybrid neuroblastoma cells causes an increase PLAPLT activity, we postulated that Atp8a1 functions as PLAPLT only in fast dividing cells, such as neurotumor cells or neuroblasts. This study used the fluorescent PS analogue, NBD-PS, to show that ectopic expression of Atp8a1 in the N18 neurotumor

Vmax for this enzyme, which suggests that overexpression of Atp8a1 causes an increase in the PLAPLT molecules. This indicates that Atp8a1 is possibly identical to the PLAPLT molecule of the N18 cells. As a confirmation of this hypothesis we expressed phosphorylation-site mutants of Atp8a1 in the N18 cells to elicit a decrease in the Vmax value of PLAPLT, without significantly altering the Km value. The inhibition of the PLAPLT activity in N18 cells was also evidenced by a striking increase in surface staining of these cells with the PS-binding protein annexin V. According to our postulate Atp8a1 deletion should also cause PS exposure in neuroblasts harbored within the dentate gyrus (DG), which is a proliferative niche within the memory center termed hippocampus. In corroboration, we observed pronounced annexin V staining in both dissociated DG cells as well as cultured hippocampal slices of Atp8a1 (-/-) mice but not wild type mice. Such PS externalization should trigger phagocytosis of DG cells, which in turn could lead to a loss of hippocampal function. In support of this postulate we have observed that the Atp8a1 (-/-) mice suffer from possibly hippocampal-related learning defects. Therefore, Atp8a1 may play a crucial role in the maintenance of the functional integrity of the hippocampus. Additionally, our study reveals a potential strategy for the selective removal of the brain tumor cells through targeted suppression of Atp8a1 activity in brain cancer cells, which would lead to PS externalization and elimination of the cells by phagocytosis.

I dedicate this thesis with love to Mami and Papi for all they have done to give me an education and a better life. You both made it possible for me to complete my thesis and come this far in life.

ACKNOWLEDGEMENTS

This thesis could not be brought to a thesis stopping point without the efforts of hardworking and dedicated people. I would like to thank all the members of the Biochemistry doctoral program at the City University of New York Graduate Center for all their support. Also, I would like to thank the Alliance for Graduate Education and the Professoriate (AGEP) program, the Louis Stokes Alliance for Minority Participation (LS-AMP) program of the City University of New York, and the National Institute of Health (NIH) minority supplement for supporting this project. A very special thanks to my mentor Dr. Probal Banerjee without whose support, encouragement and guidance the completion of this project could not have been possible. Also, I offer my sincere gratitude to the members of the supervisory committee for their guidance and advise. I would also like to thank the Project Administrator of the LS-AMP program Dr. Brathwaite and the Director of the Collegiate Science and Technology Entry Program (C-STEP) from the College of Staten Island Ms. Evans-Greene for their encouragement and support throughout my graduate studies. Special thanks also to all the members of Dr. Banerjee's lab, especially to my very good friend Sudarshana from whom I have learned and continue to learn. Also, very special thanks to my friends and lab partners Priya, Shawn, Amit and Jason for all their support. Last but not least, I want to thank my best friend Buddi for all his support throughout these five years.

Finally, I would like to thank my parents who have demonstrated their own loving patience with their still-growing daughter through the years. I would also like to thank my loving grandmother, without her I will not be the person I am today.

Table of Contents

List of Tables and Figures

ABBREVIATIONS

ABC	ATP-binding cassette
ABD	7-amino-2,1,3-benzoxadiazol-4-yl
Apaf-1	apoptotic protease activating factor-1
DISC	death-inducing signaling complex
DMEM	Dulbecco's Modified Eagles Medium
FADD	Fas-associated death domain
FBS	fetal bovine serum
GAS6	growth arrest-specific gene 6
ICAM3	intercellular adhesion molecule-3
LPC	lysophosphatidylcholine
mGBSS	modified Gey's balanced salt solution
NBD-PS	1-Oleoyl-2-[6-[(7-nitro-2-1,3-benzoxadiazol-4-yl)amino]hexanoyl]-sn-Glycero-3-Phospho-L-Serine
PC	phosphatidylcholine
PE	phosphatidylethanolamine
PM-APLT	Plasma Membrane Aminophospholipid Translocase
PMSF	phenylmethylsulfonyl fluoride
PS	phosphatidylserine
SM	sphingomylein
TRAIL	Tumor necrosis factor (TNF)-related apoptosis-inducing ligand

CHAPTER 1

INTRODUCTION

1.1 Apoptosis and Phagocytosis:

Apoptosis, the most extensively studied form of cell death, is crucial to the homeostatic regulation and survival of multicellular organisms. Apoptosis occurs during development, such as in the homeostatic turnover of cells in various tissues, "during infections and wound healing, and disease states" (Ravichandran 2007). Apoptosis can be divided into two primary phases: the signaling phase (caspase activation, DNA fragmentation and cell shrinkage) and the cell removal phase. The latter is a crucial event that prevents rupture of dying cells, activation of the immune response, and proliferation of unwanted cells.

The signaling phase of apoptosis can be divided into two pathways: extrinsic and intrinsic. In the extrinsic pathway, apoptosis is initiated through the activation of the death receptors or proapoptotic receptors: Fas, tumor necrosis factor, and TRAIL (tumor necrosis factor (TNF)-related apoptosis-inducing ligand). This is followed by the clustering and recruitment of adapter protein Fas-associated death domain (FADD) and procaspases 8 or 10 forming a death-inducing signaling complex (DISC) (Wang 2001, Kischkel 1995, Chinnaiyan 1995) leading to the activation of downstream caspases 3, 6, and/or 7. On the other hand, the intrinsic pathway is initiated by cellular signals resulting from hypoxia, defective cell cycle, DNA damage, or other cell stresses. In this pathway, pro-apoptotic proteins increase the permeability of the mitochondrial membrane leading to the release of cytochrome c. The pro-apoptotic proteins are members of the Bcl-2

superfamily of proteins, which are divided into two groups: those with a BH3 domain (Bid, Bad, Bim, Bmf, PUMA, and NOXA), and those with several BH domains (Bax and Bak) (Coultas 2003, Ashkenazi 2008). Released cytochrome c together with the adaptor apoptotic protease activating factor-1 (Apaf-1) and procaspase 9 form the apoptosome, a multiprotein complex that activates caspases 3, 6, and/ or 7 (Bao 2007, Henry-Mowatt 2004). Both, extrinsic and intrinsic pathways, lead to the activation of caspases 3, 6 and/or 7, the executionists of apoptotic signals inside the cell. They destroy essential cellular proteins, leading to controlled cell death.

The efficiency of the cell removal phase by the process of phagocytosis is crucial for "protecting tissue from harmful exposure to the inflammatory and immunogenic contents of dying cells" (Maderna 2003). Phagocytosis was first described by the Russian biologist Ilya Metchnikoff in the late 19th century (Krysko 2006). Professional phagocytes (monocytes, macrophages, dendritic cells, and mast cells) and nonprofessional phagocytes (hepatocytes, endothelial cells, epithelial cells, glomerular mesangial cells, and fibroblasts) (Hart 2008) mediate the apoptotic cell clearance phase, which can be divided into three steps: sensing and recognition of the apoptotic cell, engulfment and degradation, and the post-engulfment response of the phagocyte (Ravichandran 2007). It is known that degradation of apoptotic cells occurs rapidly; hence it is evident that necessary signals must be released at the early stages of apoptosis to bring phagocytes to close proximity of the apoptotic cell. Such signals termed 'FIND-ME' signals, include LPC (lysophosphatidylcholine) identified by Lauber *et al.,* and nucleotides (ATP and UTP) (Ravichandran 2007). The exact mechanism by which the signals are released and how they diffuse to attract phagocytes still remains elusive. Upon

attracting phagocytes, apoptotic cells undergo changes to produce recognition signals, these "EAT-ME" signals, which "are displayed on the surface of dying cells very early in the apoptotic process" (Ravichandran 2007), include externalization of phosphatidylserine (PS) in the outer layer of the plasma membrane, glycosylation (addition of sugars such as galactose, mannose, and N-glucosamine) of proteins and lipids, binding of thrombospondin to sulfated glycolipids, and expression of ICAM3 (intercellular adhesion molecule-3) and oxidized LDL-like moiety (Ravichandran 2007, Kerr 1972, Fadok 1999) .

1.2 Phosphatidylserine and plasma membrane asymmetry:

Phosphatidylserine (PS) exposure is the best-studied 'EAT-ME' signal. PS, which is normally present in the inner leaflet of the plasma membrane, reorients to the outer leaflet (Martin 1995, Fadok 1992) where it is recognized "as a naked lipid or in combination with" bridging molecules by phagocyte receptors. These bridging molecules include growth arrest-specific gene 6 (GAS6) and protein S (Ravichandran 2007, Anderson 2003, Nagata 1996).

The asymmetrical distribution of phospholipids in the plasma membrane has been extensively studied. As mentioned above, phosphatidylserine and phosphatidylethanolamine (PE) are mainly located in the cytosolic leaflet, while phosphatidylcholine (PC), sphingomylein (SM) and glycosphingolipids, reside in the outer leaflet (Ikeda 2006). This distribution is possible because phospholipids are practically unable to flip-flop through the hydrophobic membrane interior due to their polar headgroups. Consequently, such phospholipid translocation across the lipid bilayer

is a slow process requiring several hours to days (Lenoir 2007, Devaux 1992). Nonetheless, a protein or proteins or 'flippases' as described by Mark Bretscher in 1972, powers the unfavorable translocation or migration of phospholipids to maintain their asymmetry in the plasma membrane.

As mentioned earlier, during apoptosis, the asymmetry of the membrane gets compromised, bringing PS to the outer leaflet and exposing it to phagocytic cells. The exact mechanism that causes PS externalization is still unknown. Currently there are three proposed mechanisms by which PS-exposure can be regulated in the plasma membrane. These mechanisms include the three families of enzymes that maintain the asymmetric distribution of phospholipids: scramblases, floppases and flippases. Scramblases that are activated by Ca^{2+} play an important role in platelet activation and apoptosis. Rather than assisting, scramblases disrupt membrane asymmetry by ATP-independent bidirectional transportation of phospholipids across the membrane. The loss of plasma membrane asymmetry causes PS externalization, which has been shown to cause activation of blood clotting factors and recognition of macrophage (Pomorski 2001, Daleke 2003).

The other family of translocases, floppases, conducts an outward ATP-dependent translocation of phospholipids. These include the ABC (ATP-binding cassette) transporter family. There are conflicting data on the identity of the floppases that are involved in the outward movement of PS. The inward translocation of aminophospholipids is due to the activity of the third family of enzymes, aminophospholipid translocases (APLTs). The proteins in this family selectively translocate, in an ATP-dependent manner, PS and PE from the outer to the inner leaflet of

the plasma membrane. Inactivation of these proteins during apoptosis could lead to PS externalization. The exact protein or proteins responsible for the plasma membrane APLT activity has not yet been identified (Ravichandran 2007, Kerr 1972, Fadok 1999).

1.3 Aminophospholipid Translocase activity and P-Type ATPases:

In 1984, the first evidence for the involvement of a membrane protein in the maintenance of phospholipid asymmetry was demonstrated by Seigneuret and Devaux (Seigneuret 1984). Their experiment showed the specific inward movement of spin-labeled analogs of phosphatidylserine in human erythrocyte membranes. Other researchers replicated their results using fluorescent (Connor 1988) and radiolabeled (Tilley 1986) phosphatidylserine analogs (Bevers 1999). This membrane protein was shown to be specific for aminophospholipids; thus, it was referred to as 'aminophospholipid translocase' (APLT). In 1986, Zachowski *et al* showed that PS and PE were specific substrates for this transporter (Zachowski 1986). The APLT or APLT activity is ATP-dependent, consuming one molecule of ATP for each molecule of phospholipid transported (Beleznay 1993). In a query to identify the protein responsible for the APLT activity, Auland et al. purified and reconstituted a 110-kDa, Mg^{2+}-dependent ATPase from human erythrocyte membranes. In 1996 Tang and coworkers (Tang 1996) cloned the cDNA of a Mg^{2+}-ATPase II (presently named as Atp8a1) from bovine chromaffin granules, which was previously shown to require PS to be fully active (Moriyama 1988).

The ATPase activity of this Mg^{2+}-ATPase II or Atp8a1 is vanadate and N-ethylmaleimide (NEM) sensitive, just as the APLT activity was shown to be. It has been

purified from different sources, including chromaffin granules, clathrin-coated vesicles, and plasma membrane of erythrocytes (Ding 2000). Atp8a1 is a member of the fourth subfamily of P-type ATPases, which includes five yeast and fourteen human members. Atp8a1 is homologous to a TGN-resident protein in yeast encoded by the *drs2* gene (Lenoir 2007) and to the C. *elegans* Tat-1protein (Zullig 2007, Darland-Ransom 2008b) . Although there are controversies with the Drs2p-mediated plasma membrane NBD-PS translocation activity, Atp81 and Drs2p were the first members of the type IV subfamily of P-type ATPases, also known as putative APLTs.

The expected structure of P-Type ATPases consists of ten transmembrane domains with the amino- and carboxy-termini extending toward the cytoplasm. The P-type ATPase-specific sequences and an ATP-binding site are located in the large intracellular loop. One of the P-type ATPase-specific sequences is known as the P-signature sequence, 'DKTGT[L,I,V,M][T,I,S]'. The aspartic acid residue in this sequence is essential for the phosphorylation/dephosphorylation reaction of the enzyme. Studies have shown that mutation of this residue impairs the ATPase activity of the enzyme without affecting substrate or ATP binding. In the mechanism by which P-type ATPases translocate their substrates across a membrane, at least four conformational changes occur to cause this translocation. Upon binding of a substrate (ion 1), a conformational change occurs causing phosphorylation of the enzyme by Mg^{2+}-ATP at the aspartic acid residue. The phosphorylated enzyme increases its affinity for a second substrate (ion 2), while releasing the first ion on the other side of the membrane. The binding of the second substrate causes another conformational change triggering the hydrolysis of the aspartic acid-phosphate. A third conformational change occurs leading to the release of the

second substrate. The enzyme increases its affinity for the first ion starting the cycle again (Kuhlbrandt 2004) (Figure 1).

In type-IV P-type ATPases, found only in eukaryotes, the metal interacting amino acids in transmembrane domains 4 and 6 of most cation-transporting P-type ATPases are replaced by hydrophobic amino acids (Kuhlbrandt 2004). The phylogenetic relationship between members of this subfamily is shown in Figure 2. The closest paralog of Atp8a1 (U75321) is Atp8a2 (AF156550), which is also a putative flippase with 67% sequence identity with Atp8a1 (Figure 3).

1.4 Atp8a1

Atp8a1 has been the candidate for the plasma membrane APLT for many years. Most of what is known about the APLT activity and Atp8a1 has been established in human erythrocytes, yeast and recently in C. *elegans*. No studies have been previously done in mouse neuronal cells or cancer cells. mRNA expression of Atp8a1 is high in mouse **brain**, heart, and lung. In the mouse brain, Atp8a1 mRNA is highly expressed in the basal forebrain, amygdala and hippocampus (Halleck 1999).

OBJECTIVE OF THIS STUDY

Our goal was to understand the role of Atp8a1 as the plasma membrane aminophospholipid translocase (PM-APLT) of the neuroblastoma cell line N18 and of proliferating neuroblasts of the hippocampus.

In this project, we provide evidence showing that Atp8a1 is the PL-APLT of the neuroblastoma cell line N18. This is demonstrated through kinetic analysis of plasma membrane APLT activity after overexpression of Atp8a1 or suppression of its activity by using phosphorylation-site mutants. Furthermore, the effect of the absence of Atp8a1 on PS exposure in proliferating brain cells is tested in an Atp8a1 (-/-) mouse line.

Figure 1: P-type ATPases ion-translocation cycle. The process starts in the E1 state with the binding of ion 1 (X^+) to its high-affinity site in the membrane (M) domain from the cytoplasm, and the binding of Mg^{2+}-ATP to the nucleotide-binding pocket (N). The protein then moves into the E1-P conformation in which the Mg^{2+}-ATP is brought close to the phosphorylation domain (P, green). This results in phosphorylation of the Asp residue in the P-type signature domain. The protein enters E2-P conformation in which the TGE-containing face of the actuator domain (A, orange) is oriented toward the phosphorylation site where it binds to the Mg^{2+}-ADP product leading to expulsion of the ADP molecule produced in the reaction and also ejection of the X^+ ion into the extracellular fluid. The E2 state is set by the influx of ion 2 (Y^+) triggering hydrolysis and releasing the phosphate and Mg^{2+} ions. The A domain reorients and the molecule returns back to the E1 state (Kühlbrandt 2004).

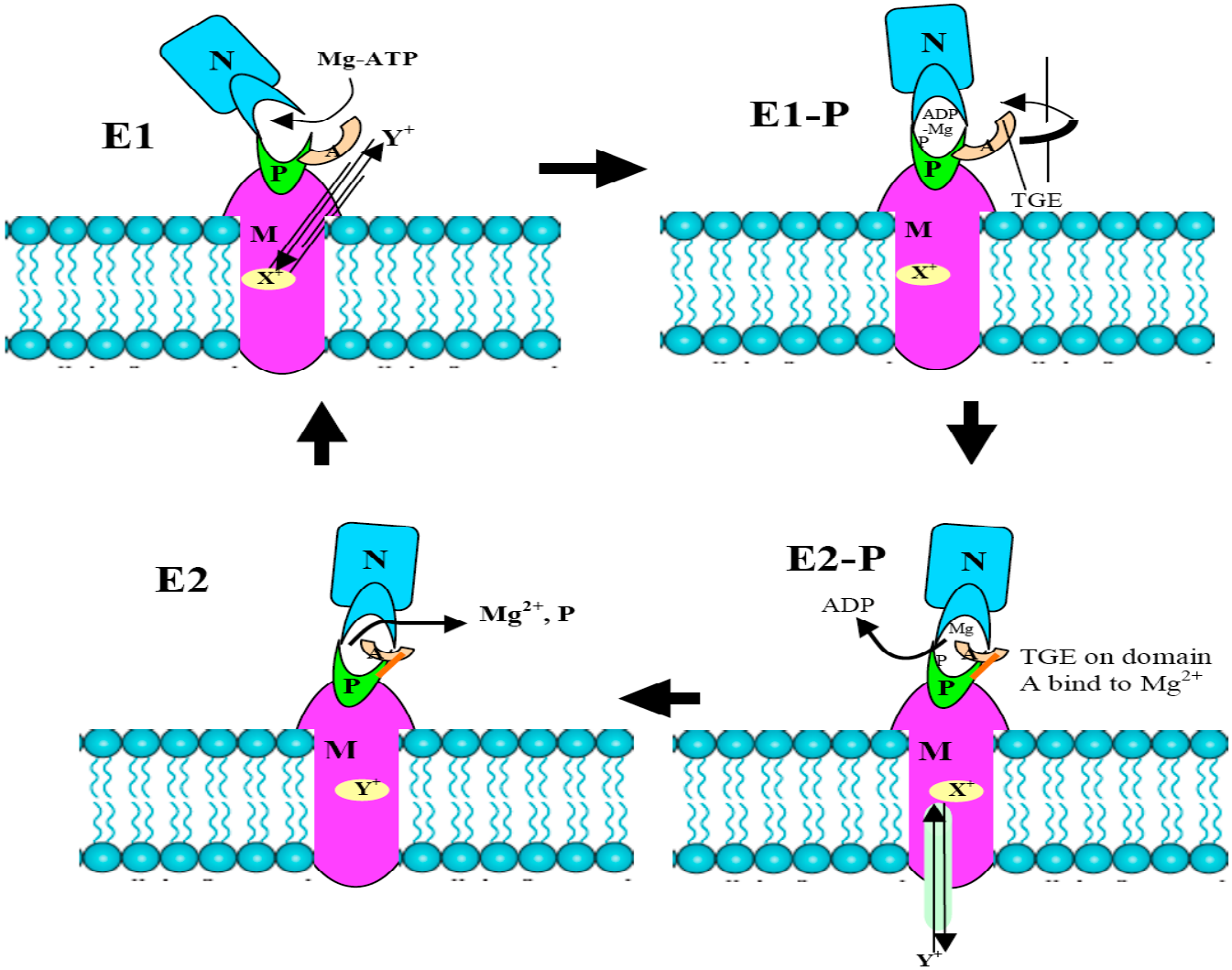
E1
N
Mg-ATP
P
A
Y^+
M
X^+
E1-P
N
ADP
-Mg
P
P
A
TGE
M
X^+
E2-P
N
ADP
Mg
P
P
A
TGE on domain
A bind to Mg^{2+}
M
X^+
Y^+
E2
N
Mg^{2+}, P
P
A
M
Y^+

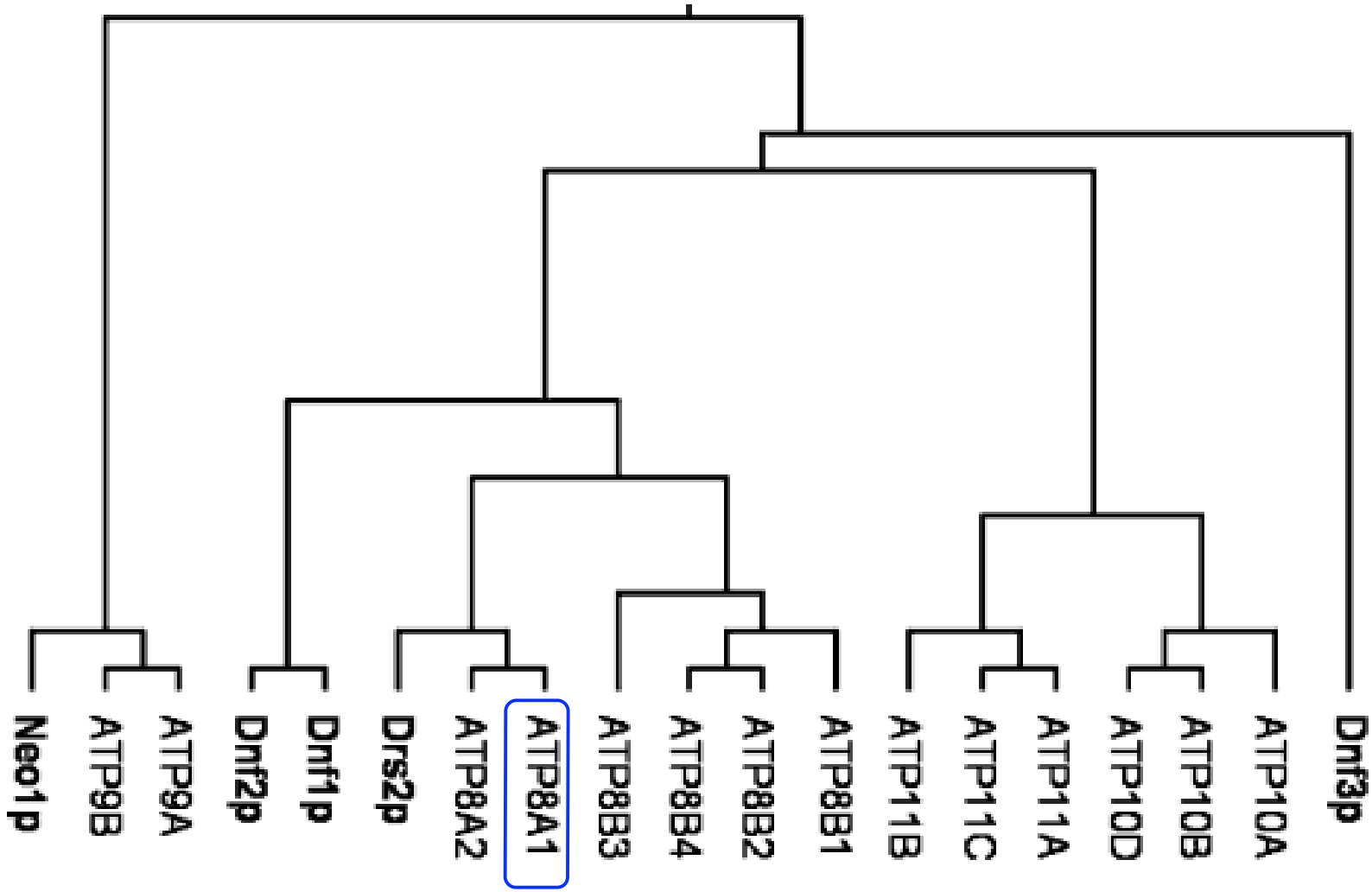

Figure 2: Phylogenetic analysis of the human and yeast Saccharomyces cerevisiae (in bold) type 4 ATPases (Paulusma 2005)

Figure 3: Amino acid sequence alignment between Atp8a1 (accession number NM_009727) and Atp8a2 (accession number AF156550) shows a 67% sequence identity between the two type-IV P-type ATPases. The alignment between the two amino acid sequences was done using blast (http://blast.ncbi.nlm.nih.gov/Blast).

Atp8a1 and Atp8a2 amino acid sequence comparison

```
Atp8a1   24   VSEKTSLADQEEV--RTIFINQPQLTKFCNNHVSTAKYNVITFLPRFLYSQFRRAANSFFLFIALLQQIP   91
              +S  TS+ DQ E   R I++NQ  L KFC+N +STAKY+V+TFLPRFLY Q RRAAN+FFLFIALLQQIP
Atp8a2   1    MSRATSVGDQLEAPARIIYLNQSHLNKFCDNRISTAKYSVLTFLPRFLYEQIRRAANAFFLFIALLQQIP   70

Atp8a1   92   PDVSPTGRYTTLVPLLFILAVAAIKEIIEDIKRHKADNAVNKKQTQVLRNGAWEIVHWEKVNVGDIVIIKG 161
              PDVSPTGRYTTLVPL+ IL +A IKEIIED KRHKADNAVNKK+T VLRNG W  + W++V VGDIV +
Atp8a2   71   PDVSPTGRYTTLVPLVIILTIAGIKEIIEDFKRHKADNAVNKKKTIVLRNGMWHTIMWKEVAVGDIVKVLN 140

Atp8a1   162  KEYIPADTVLLSSSEPQAMCYIETSNLDGETNLKIRQGLPATSDIKDIDSLMRISGRIECESPNRHLYDF  231
               +Y+PAD VL SSSEPQ MCY+ET+NLDGETNLKIRQGL  T+D++  D LM++SGRIECE PNRHLYDF
Atp8a2   141  GQYLPADMVLFSSSEPQGMCYVETANLDGETNLKIRQGLSHTTDMQTRDVLMKLSGRIECEGPNRHLYDF  210

Atp8a1   232  VGNIRLDGHGTVPLGADQILLRGAQLRNTQWVHGIVVYTGHDTKLMQNSTSPPLKLSNVERITNVQILIL  301
               GN+ LDG  +V LG DQILLRG QLRNTQWV G+VVYTGHD+KLMQNST  PLK SNVE++TNVQIL+L
Atp8a2   211  TGNLHLDGKSSVALGPDQILLRGTQLRNTQWVFGVVVYTGHDSKLMQNSTKAPLKRSNVEKVTNVQILVL  280

Atp8a1   302  FCILIAMSLVCSVGSAIWNRRHSGKDWYLHLHYGGASNFGLNFLTFIILFNNLIPISLLVTLEVVKFTQA  371
              F IL+ M+LV SVG+  WN  H GK WY+      + NFG N LTFIIL+NNLIPISLLVTLEVVK+TQA
Atp8a2 281   FGILLVMALVSSVGALFWNGSHGGKSWYIKKMDTNSDNFGYNLLTFIILYNNLIPISLLVTLEVVKYTQA  350

Atp8a1   372  YFINWDLDMHYEPTDTAAMARTSNLNEELGQVKYIFSDKTGTLTCNVMQFKKCTIAGVAYGQSSQFGDEK  441
               FINWD+DM+ Y  DT AMARTSNLNEELGQVKY+FSDKTGTLTCN+M FKKC+IAGV YG   +   E+
Atp8a2   351  LFINWDMDMY YIENDTPAMARTSNLNEELGQVKYLFSDKTGTLTCNIMNFKKCSIAGVTYGHFPELAREQ 420
```

Figure 3 (continued)

```
Atp8a1  442  T----------------FNDPSLLDNLQNNHPTAPIICEFLTMMAVCHTAVPEREGDKIIYQAASPDEGA  495
             +                 FNDP LL N+++ HPTAP I EFLT++AVCHT VPE++GD+IIYQA+SPDE A
Atp8a2  421  SSDDFCRMTSCTNDSCDFNDPRLLKNIEDQHPTAPCIQEFLTLLAVCHTVVPEKDGDEIIYQASSPDEAA  490

Atp8a1  496  LVRAAKQLNFVFTGRTPDSVIIDSLGQEERYELLNVLEFTSARKRMSVVVRTPSGKLRLYCKGADTVIYE  565
             LV+ AK+L FVFTGRTP SVII+++GQE+ + +LNVLEF+S RKRMSV+VR PSG+LRLYCKGAD VI+E
Atp8a2  491  LVKGAKKLGFVFTGRTPYSVIIEAMGQEQTFGILNVLEFSSDRKRMSVIVRLPSGQLRLYCKGADNVIFE  560

Atp8a1  566  RLAETSKYKEITLKHLEQFATEGLRTLCFAVAEISESDFEEWRAVYHRASTSVQNRLLKLEESYELIEKN  635
             RL++ SKY E TL HLE FATEGLRTLC A A++SE+++EEW  VY  AS  +++R  +LEE YE+IEKN
Atp8a2  561  RLSKDSKYMEETLCHLEYFATEGLRTLCVAYADLSENEYEEWLKVYQEASIILKDRAQRLEECYEIIEKN  630

Atp8a1  636  LQLLGATAIEDKLQDQVPETIETLMKADIKIWILTGDKQETAINIGHSCRLLKRNMGMIVINEGSLDGTR  705
             L LLGATAIED+LQ  VPETI TL+KA+IKIW+LTGDKQETAINIG+SCRL+ +NM +I++ E SLD TR
Atp8a2  631  LLLLGATAIEDRLQAGVPETIATLLKAEIKIWVLTGDKQETAINIGYSCRLVSQNMALILLKEDSLDATR  700

Atp8a1  706  ETLSRHCTTLGDALRKENDFALIIDGKTLKYALTFGVRQYFLDLALSCKAVICCRVSPLQKSEVVEMVKK  775
               +++HCT LG+ L KEND ALIIDG TLKYAL+F VR+ FLDLALSCKAVICCRVSPLQKSE+V++VKK
Atp8a2  701  AAITQHCTDLGNLLGKENDVALIIDGHTLKYALSFEVRRSFLDLALSCKAVICCRVSPLQKSEIVDVVKK  770

Atp8a1  776  QVKVITLAIGDGANDVSMIQTAHVGVGISGNEGLQAANSSDYSIAQFKYLKNLLMVHGAWNYNRVSKCIL  845
             +VK ITLAIGDGANDV MIQTAHVGVGISGNEG+QA N+SDY+IAQF YL+ LL+VHGAW+YNRV+KCIL
Atp8a2  771  RVKAITLAIGDGANDVGMIQTAHVGVGISGNEGMQATNNSDYAIAQFSYLEKLLLVHGAWSYNRVTKCIL  840
```

Figure 3 (continued)

```
Atp8a1   846  YCFYKNIVLYIIEIWFAFVNGFSGQILFERWCIGLYNVMFTAMPPLTLGIFERSCRKENMLKYPELYKTS  915
               YCFYKN+VLYIIE+WFAFVNGFSGQILFERWCIGLYNV+FTA+PP TLGIFERSC +E+ML++P+LY+ +
Atp8a2   841  YCFYKNVVLYIIELWFAFVNGFSGQILFERWCIGLYNVIFTALPPFTLGIFERSCTQESMLRFPQLYRIT  910

Atp8a1   916  QNALDFNTKVFWVHCLNGLFHSVILFWFPLKALQYGTVFGNGKTSDYLLLGNFVYTFVVITVCLKAGLET  985
               QNA  FNTKVFW HC+N L HS+ILFW P+KAL++ T   +G  +DYL +GN VYT+VV+TVCLKAGLET
Atp8a2   911  QNAEGFNTKVFWGHCINALVHSLILFWVPMKALEHDTPVTSGHATDYLFVGNIVYTYVVVTVCLKAGLET  980

Atp8a1   986  SYWTWFSHIAIWGSIALWVVFFGIYSSLWPAVPMAPDMSGEAAMLFSSGVFWVGLLSIPVASLLLDVLYK  1055
               + WT FSH+A+WGS+ +W+VFFG+YS++WP +P+APDM+A   M+ SS  FW+GL  +P A L+ DV ++
Atp8a2   981  TAWTKFSHLAVWGSMLIWLVFFGVYSTIWPTIPIAPDMKGQATMVLSSAYFWLGLFLVPTACLIEDVAWR  1050

Atp8a1  1056  VIKRTAFKTLVDEVQELEAKSQDPGAVVL----GKSLTERAQLLKNVFKKNHVNLYRSESLQQNLLHGYA 1121
                 K T  KTL++EVQELE KS+  G  +L    GK + ER +L+K + +K    L+R+ S+QQ + HGYA
Atp8a2  1051  AAKHTCKKTLLEEVQELETKSRVMGKAMLRDSNGKRMNERDRLIKRLSRKTPPTLFRTGSIQQCVSHGYA  1120

Atp8a1  1122  FSQDENGIVSQSEVIRAYDTTKQ 1144
               FSQ+E+G V+Q E++RAYDTTK+
Atp8a2  1121  FSQEEHGAVTQEEIVRAYDTTKE 1143
```

CHAPTER 2

MATERIALS AND METHODS

2.1 Reagents:

For immunoblotting or immunohistochemistry analysis, the following antibodies were used: Monoclonal Anti-β-Actin antibody (Sigma, MO, USA), Ab-B (Ding 2000), custom made Atp8a2 antibody (Aves Labs Inc, OR, USA), goat anti-mouse IgG-HRP and anti-rabbit IgG-HRP antibodies (Santa Cruz Biotechnology Inc, CA, USA), Alexa Fluor 488 goat anti-rabbit IgG and Alexa Fluor 488 goat anti-mouse IgG (Invitrogen Corporation, CA, USA). For PCR and cloning, the following reagents were used: the TOPO-TA™ Cloning Kit, the THERMOSCRIPT™ RT-System, the Platinum® Taq High Fidelity thermostable DNA polymerase, agarose and dNTPs mixture (Invitrogen Corporation, CA, USA). The QIAprep Miniprep plasmid DNA isolation kit, QIAquick PCR purification kit, QIAquick gel extraction kit, RNeasy Mini kit including QIAShredder™ columns and on-column DNase digestion kit were purchased from (QIAGEN, CA, USA). For genotyping, Proteinase K (Invitrogen Corporation, CA, USA) was used. For promoter analysis, the pGL3-Basic (no promoter) and pGL3-Promoter (SV40 promoter) firefly luciferase reporter plasmids, pRL-TK vector and the Dual Luciferase Reporter (DLR) assay kit (Promega, WI, USA).

2.2 Animals:

C57 mouse was used for gDNA and RNA isolation. Mice were obtained from Taconic and kept in the CSI Animal Facility. Atp8a1 (+/-) mice were purchased from Jackson Laboratories and then bred and genotyped to obtain Atp8a1 (-/-) mice.

2.3. Cell lines

For our experiments, the following cell lines were used: mouse neuroblastoma cell line N18 (generously provided by Dr. Efrain Azmitia, New York University, NY), mouse hippocampal neuron-derived hybrid neuroblastoma cell line HN2 (obtained from the CSI cell depository), mouse melanoma cell line B16F10 (generously provided by Dr. Susan Rotenberg, Queens College, NY). All cells were cultured in DMEM (Dulbecco's Modified Eagles Medium) containing 10% FBS (Fetal Bovine Serum) and 1% PS (Penicillin–Streptomycin). NIH3T3 cell line (generous gift from Dr. Yu-Wen Hwang's lab at the NY State Institute For Basic Research, Staten Island, NY) were cultured with DMEM media containing 10% Calf Serum and 1% PS.

2.4 Atp8a1 and Atp8a2 expression vectors:

Mouse brain RNA was isolated using the RNeasy Mini Kit (QIAGEN, CA, USA) and the cDNA was obtained by using ThermoScript™ RT-PCR System plus Platinum® Taq DNA Polymerase (Invitrogen Corporation, CA, USA). For amplification of Atp8a1 or Atp8a2, primers were designed with the addition of restriction sites for directional cloning (Table 1). The downstream primer (the antisense primer) included the coding sequence but not the stop codon, to allow insertion into pCDNA6.1/ myc-HisA (for

Atp8a1) and/or pcDNA6.1/ myc-His C (for Atp8a2) in-frame with the *myc*-His sequences to eventually achieve expression of epitope-tagged Atp8a1 and Atp8a2.

2.5 Phosphorylation-site mutant construct of Atp8a1:

The aspartate residue in the P-type signature sequence '**D**KTGTL' was mutated to either lysine (D409⇨K) or glutamate (D409⇨E) using the GeneTailor™ Mutagenesis System (Invitrogen, CA, USA) as previously described in Levano *et al*. (Levano *et al.* 2009). Briefly, Atp8a1-pcDNA6/*myc*-His A construct was first methylated and PCR amplified using two overlapping primers (Table 1). As shown in Figure 4, one of the two primers contained the required mutation **(D409K)** or **(D409E)** in order to produce the desired mutation within the '**DKTGTL**' motif. The PCR product was transformed into mcrBC^{+} E.coli. Unmutated, methylated parent plasmid was digested in the mcrBC^{+} *E.coli* and only the mutated plasmid was obtained after lysis and DNA isolation.

						397				**409**					
amino acid:	L	G	Q	V	K	Y	I	F	S	D	K	T	G	T	L
cDNA:	CTTGGCCAGGTTAAATACATATTTTCTGACAAAACTGGGACCCTG														

Figure 4: Fragment of the amino acid and cDNA sequences of the Mus *musculus* Atp8a1. Underlined is the DKTGTLT sequence motif.

2.6 Transfection of cells with plasmid DNA:

Tumor cells, plated in poly-L-lysine-coated six-well plates, were allowed to grow up to 60% confluency. For the non-tumor cells, which were differentiated after transfection, were allowed to grow up to 70-80% confluency. At this point, the cells were transfected as described here. The plasmid DNA (3 µg) was diluted in 200 µl 150 mM NaCl (for all the tumor cells) and the mixture was gently vortexed and spun briefly. Next, ExGen transfection reagent (Fermentas, Inc., MD), at 7:1 molar equivalent ratio for amine in polyethyleneimine (in the reagent) vs DNA, was added to the DNA solution. This amounts to 11.52 µl of the reagent per sample per well. For HN2 cells, the DNA was dissolved 100 µl of 5% glucose and then the ExGen reagent, adjusted to 100 µl with 5% glucose, was added to the DNA solution. The mixture was vortexed for 10 s and then incubated for 10 min at room temperature. The medium in each well of cells was replaced with 1.8 ml of serum-free DMEM and then the 200 µl of DNA-ExGen complex was added to it, followed by gentle rocking to achieve even distribution of the complex. For cotransfection of pEGFP or pAsRed2-N1, 2.4 µg of the experimental plasmid was mixed with 0.6 µg of pEGFP or pAsRed2-N1 in 200 µl of 5% NaCl or 5% glucose. Typically, the cells were allowed to incubate for three hours in a 37-°C CO_2 incubator, following which fetal bovine serum (FBS) was added to each well to a final concentration of 10%, and then the cells were allowed to incubate overnight in the incubator. The medium was then changed to DMEM containing 10% FBS and 1% Pen-Strep for tumor cells or the differentiation medium and the cells visualized using fluorescence microscopy for transfection. Differentiation of the HN2 and SN48 cells was achieved in 1% serum-containing DMEM containing 5 µM retinoic acid. Control wells were

transfected with the same amount of empty vector, which, in this case, was pCDNA6.1.

2.7 Aminophospholipid translocase assay:

The APLT activity of the plasma membrane was measured in cells using NBD-PS (1-Oleoyl-2-[6-[(7-nitro-2-1,3-benzoxadiazol-4-yl)amino]hexanoyl]-sn-Glycero-3-Phospho-L-Serine) (Avanti Polar Lipids, Inc.) by modifying reported procedures (Tyurina 2007, McIntyre 1991, Connor 1992). All assays were completed using triplicate samples.

For the **time-course APLT assays**, briefly, cells (~10^6) were washed and resuspended in 1 ml ice-cold incubation buffer (136 mM NaCl, 2.7 mM KCl, 2 mM MgCl2, 5 mM glucose, 10 mM HEPES, 500 µM PMSF, pH 7.5). Cells were then incubated with NBD-PS (10µM; dissolved in 12 µl of ethanol) on ice for 10 min allowing incorporation of NBD-PS to the outer leaflet of the plasma membrane, while preventing translocation and endocytosis. Unbound NBD-PS was then removed by washing the cells with ice-cold incubation buffer. Cells were resuspended in 1 ml ice-cold incubation buffer and incubated at 28 °C for 0, 5, 10 and 15 min, allowing translocation of PS (NBD-PS). Untranslocated NBD-PS fluorescence remaining in the outer leaflet of the plasma membrane was removed by modifying NBD (7-nitro-2,1,3-benzoxadiazol-4-yl) to the non-fluorescent fluorophore ABD (7-amino-2,1,3-benzoxadiazol-4-yl) (McIntyre 1991) by incubating the cell suspension with sodium dithionite ($S_2O_4^{-2}$; 10mM) for 30 s on ice. Cells were then washed and resuspended in 220 µl of 1X PBS. For fluorescence analysis using a fluorescence plate reader (FLX800) set at excitation and emission wavelengths of 485 nm and 530 nm, the cell suspension (200 µl sample) was placed in a

well of a 96 well-plate. For microscopy, cells were resuspended in mounting medium and placed on a slide (Figure 5).

For the **substrate concentration-dependant APLT assays**, cells (~10^6) were washed and resuspended in 1 ml ice-cold incubation buffer. Increasing concentrations of NBD-PS in 12 µl ethanol (ice-cold) were then added to the 1 ml cell suspension to obtain the following concentrations: (in µM) 0.35, 0.5, 0.75, 1, 2, 4. The cell suspension was incubated for 10 min on ice. Cells were then washed, resuspended in 1 ml ice-cold incubation buffer, and incubated at 28 °C for 10 min (time at which translocation is in the linear range). After the 10 min incubation, the cell suspension was placed back on ice. NBD-PS fluorescence remaining in the outer leaflet of the plasma membrane was removed by incubating the cell suspension on ice with sodium dithionite (10 mM) for 30 s. Cells were then washed and resuspended in 220 µl of 1X PBS. 200 µl of each cell suspension was placed in a well of a 96-well plate for fluorescence analysis using a fluorescence plate reader as stated before.

For all APLT assays, to record the background fluorescence, ~10^6 cells per sample were incubated with 12 µl of ethanol without NBD-PS and then at 28 °C for 10 min, followed by the same treatment as performed for the NBD-PS containing samples. To account for the loss of cells during the entire assay, 20 µl of each cell suspension was used to count cells (using a hemocytometer). All fluorescence values were normalized to 10^5 cells. The average of the normalized background fluorescence was subtracted from each normalized fluorescence value obtained from the NBD-PS-treated samples. For the time-course APLT assays, we plotted as fluorescence units/10^5 cells versus time (min). For the concentration-dependant APLT assays, the fluorescence values were converted to

micromole of NBD-PS by comparing with a standard curve constructed using fluorescence readings from NBD-PS/PC vesicles containing increasing concentrations of NBD-PS (in μM, 0.1, 0.5, 1, 2.5, and 5). The micromole values were then converted into NBD-PS molecules translocated by using the Avogadro number. Lineweaver-Burk plots were constructed by using V_0 in molecules/10^5 cells/min and [S] as concentrations of NBD-PS in μM.

***Determination of the actual NBD-PS concentration in the outer leaflet of the plasma* membrane :** A fourth sample was run in parallel to the substrate concentration-dependant APLT assay to account for the true NBD-PS concentration in the outer leaflet of the plasma membrane. Briefly, cells were washed, resuspended, and incubated with NBD-PS (0.35, 0.5, 0.75, 1, 2, 4 μM) as stated previously for 10 min on ice. Then, cells were washed and resuspended in 220 μl of 1X PBS. Each cell suspension (200 μl) was placed in one well of a 96 well plate and all the samples were analyzed using a fluorescence plate reader. The fluorescence values were converted to μmoles of NBD-PS by comparing with a standard curve constructed as stated previously. After finding the thickness of the plasma membrane (~6 nm) (Kuchel 1988) and the diameter of a cell in suspension (~14 μmeters) (Arms 1995) (Fig. 6), we calculated the volume of the outer leaflet of the plasma membrane (1.85 μm^3). Then, we divided the NBD-PS μM concentrations by the volume of the outer leaflet of the plasma membrane calculated (Figure 6).

2.8 Membrane isolation using the Mem-PER kit:

About 5 x 10^5 cells in microcentrifuge tubes were pelleted down, washed once with PBS and then supplemented with 150 µl of Reagent A (lysis buffer) from the Mem-Per kit (Pierce). The mixture was incubated at room temperature for 10 min and then 450 µl of Reagent B/C was added to the mixture, followed by incubation for 30 min on ice. The mixture was then centrifuged at 10,000-x g for 3 min. The supernatant, containing solubilized proteins, was separated and then incubated at 37 °C for 10 min to separate phases. Following this, the mixture was centrifuged at 10, 000 x g for 2 min. The top layer, containing the hydrophilic proteins, and the bottom layer, containing the hydrophobic membrane proteins, were separated. The fractions separated were assayed for protein and then aliquots containing equal mass of protein were resolved using SDS-PAGE and Western blotting as discussed in the following section.

2.9 SDS-PAGE and Immunoblotting analysis:

To determine the expression levels of Atp8a1, tissue and cell lysates prepared in RIPA buffer (PBS containing 1% NP40, 0.5% sodium deoxycholate, 0.1% SDS, 0.5 mM Na3VO4, protease inhibitor cocktail, PMSF) or in a buffer from the Mem-PER kit were used. Aliquots containing 50-100 µg protein were mixed with SDS-PAGE treatment buffer and boiled for 5 min. Proteins were resolved on a 7-16% gradient SDS-PAGE gel and then transferred to nitrocellulose membrane. For Atp8a1 analysis, blots were blocked overnight with 5% nonfat dry milk in 0.1% Tween-TBS and subsequently incubated overnight with Atp8a1 antibody (antibody B) (1:10,000 dilution). Following three washes with 0.1% Tween-TBS, blots were incubated for 1 h with horseradish peroxidase-labeled

goat-anti-rabbit IgG (1:20,000). Protein bands were detected using Super signal West Pico kit (Pierce). For normalization, blots were stripped using a stripping buffer (0.25M glycine, pH 2.0) for 1hr at room temperature, re-blocked and probed with monoclonal β-Actin antibody (Sigma) in a 1:10,000 dilution with overnight incubation. After subsequent washes, blots were incubated with horseradish peroxidase-labeled goat-anti-mouse IgG (1:50,000).

2.10 Annexin V staining:

Annexin V labeling of surface PS was monitored using the Vybrant® Apoptosis Assay Kit #2 – Alexa Fluor® 488 annexin V/propidium iodide (Invitrogen, CA, USA) according to the manufacturer's instructions. Briefly, cells were resuspended in 500 µl of 1X annexin-binding buffer (for slice cultures 100 µl of 1X annexin-binding buffer was used). Alexa Fluor® 488 annexin V (5µl), 100 µg/ml propidium iodide (PI) solution (1 µl) and Hoechst 33348 (1µM) were added to 100 µl of the cell suspension (or slice culture), followed by incubation at room temperature for 20 min. Cells (or slice cultures) were then washed with 1X annexin-binding buffer and mounted on slides with ProLong® Gold antifade reagent (Invitrogen, CA, USA) for visualization and photography using a fluorescence microscopy.

2.11 Genotyping to identify Atp8a1 (-/-) pups:

For mouse-tail genomic DNA extraction, a modified protocol from Molecular cloning Sambrook Russell was used. Briefly, mouse tails (about 4-mm long) were collected and lysed in SNET lysis buffer containing 20 mM Tris-Cl (pH 8), 5 mM EDTA (pH 8), 400 mM NaCl, 1% (w/v) SDS and 400 µg/ml of Proteinase K (stock 20 mg/ml). After overnight incubation at 55 °C with vigorous shaking, the tail DNA solution was incubated with phenol:chloroform:isoamyl (25:24:1) alcohol solution at room temperature for 30 min with shaking. The aqueous phase was separated and incubated with equal volume of isopropanol to precipitate the genomic DNA. DNA pellets were resuspended in 1 mM Tris HCl/ 0.1 mM EDTA. The primer sequences and strategy were obtained from the JAX labs. Three primers were used to differentiate between the Atp8a1 knockout product (437-bp) from the wild type Atp8a1 product (253-bp) gene (IMR6315: GCT GTC AAT GAT GCG CTT CCT CCT C, IMR6314: GGG CCA GCT CAT TCC TCC CAC TCA T, IMR6313: TGT TCA CAG ATC AAA AGA CCC TAT C). PCR analysis was performed in a 50 µl reaction volume containing 500 ng of extracted genomic DNA, 0.2 mM dNTP mix, 2 mM $MgSO_4$, 0.2 µM primers, and 2.0 units of Platinum® *Taq* DNA Polymerase High Fidelity (Invitrogen, CA, USA). PCR conditions were 95°C for 30 s followed by 35 cycles of denaturation at 94 °C for 30 s, annealing at 55 °C for 30 s, and extension at 68 °C for 1 min. PCR products were analyzed by 1% agarose gel electrophoresis with ethidium bromide staining in comparison to a 1-kb ladder (Invitrogen, CA, USA).

2.12 Dissociation of DG cells:

Dentate Gyrus (DG) cells were obtained from ATP8a1 KO and wild type C57BL/J6 mice. Briefly, mice were anesthetized with ketamine (100 mg/Kg) and decapitated. Under sterile conditions, the hippocampus was isolated. Transverse slices (600-µm thick) were prepared using a tissue chopper (Stoelting, IL, USA). The DG was removed from the hippocampus using the Harris Uni-Core, Hole 1.5-mm chopper (Ted Pella, Inc., CA, USA). DG slices were incubated in trypsin-EDTA (2.5 g/L) for 5 min at 37 °C. The tissue was further dissociated by gentle triturating with a pipette. Dissociated cells were centrifuged, washed once with 1X PBS, and then immediately processed for annexin V staining**.**

2.13 Organotypic culture of hippocampal slices:

This protocol has been modified from Mehta *et al* 2007 (Mehta 2007). Briefly, as stated above, the hippocampus was isolated under sterile conditions and placed in modified Gey's balanced salt solution (mGBSS) (pre-chilled to 4°C) while bubbling a mixture of 95% O_2 and 5% CO_2. Transverse slices (400-µm thick) were prepared using a tissue chopper (Stoelting, IL, USA). Slices were placed on Millicell CM filters (Millipore, MA, USA) in a six-well dish with 1 mL of medium. The slices were kept on high potassium culture medium (25% horse serum, 50% basal essential media-Eagles, 25% Earle's balanced salt solution (EBSS), 25 mmol/L Na-HEPES, 1 mmol/L glutamine, 28 mmol/L glucose, pH 7.2) for the first 2 days. After incubation at 32°C in a 5% CO_2 atmosphere, the culture medium was changed to physiological potassium slice culture medium (20% dialyzed fetal bovine serum, 5% basal essential media-Eagles, and EBSS

modified to adjust the potassium concentration to 2.66 mmol/L). After 20% dialyzed serum treatment for 2 days, slices were used for annexin V staining.

2.14 Evaluation of hippocampal function of the Atp8a1 (-/-) mice:

Briefly, to test the hippocampus dependent visual discrimination learning, the Water T-Maze was used. Briefly, the T-maze was constructed from a plastic reservoir containing a start arm (30 cm long and 15 cm wide). The exit of the start arm was located at the center of a perpendicular corridor (80 cm long and 15 cm wide) giving a left and a right arm (each of 32.5 cm long). The start arm and the perpendicular corridor were filled with water (made opaque with white Crayola non-toxic white powder paint) that was 23º C. The depth of the water was 15 cm.

Every mouse underwent training on the first day, where they were allowed to run through 10 trails. During each trial, each mouse was placed in the start arm of the T-Maze, which was filled with water. They were supposed to reach the horizontal arms where in one of the arms, at the far end, was placed a submerged platform, which acted as a reward and reinforcement for them to escape the water. There were 2 spatial cues, one in each arm and the triangle spatial cue was always supposed to be in the arm that had the submerged platform. During each trial, the platform, along with the cue, was randomly switched between the two horizontal arms. After the first training day, they underwent 8 trials everyday because it was realized from the experience on the training day that last 2 trials in a total of 10 were really exhausting for the mice. The maximum testing period was pre-decided to be 12 consecutive days. A mouse that was able to complete eight out of ten trials per day without error for four consecutive days was considered to have

learned the task. The errors charged were: (1) if the mouse entered the arm of the T-maze where the platform was not located with all four paws; (2) if the animal turned back around and re-entered the start arm. At the end, the number of days needed for each mouse to reach learning criteria was recorded and compared to assess visual discriminatory learning ability (Teather 2002, Denayer 2008).

Table 1: Primers used for site-directed mutagenesis

Vector Constructs	Name	Sequence (5'-3')	Source
Atp8a1-pcDNA6.1/*myc*-His A	Fwd-mATPase-HindIII	CCC **AAG CTT** CGA GAC CCA CCT GCA GGG GCT	NM_009727
Atp8a1-pcDNA6.1/*myc*-His A	Rvs-mATPase-SalI	TTG AC **GTC GAC** CCA CTC ATC GGG CCT CTG TTT G	NM_009727
Atp8a2-pcdDNA6.1/*myc*-His C	mATPaseIb-S-F-KpnI	CGG **GGT ACC** TCG ATT CTG CAG GAC CCG TTC G	AF156550
Atp8a2-pcdDNA6.1/*myc*-His C	mATPaseIb-S-r-Not I	ATA GTT TA **GCG GCC GC**T TTT CTT CCT TGA ATT CTC TTT GGT GGT ATC ATA AGC GCG	AF156550
Atp8a1-D409K/E	ATPASEII-D409K/E-R1	CTTGAACCGGTCCAATTTATGTATAAAAGA	NM_009727
Atp8a1-D409K	ATPASEII-D409K-F1	AAATACATATTTTCT**AA**G**G**AAAACTGGGACC	NM_009727
Atp8a1-D409E	ATPASEII-D409E-F2	AAATACATATTTTCTGA**G**AAAACTGGGACC	NM_009727

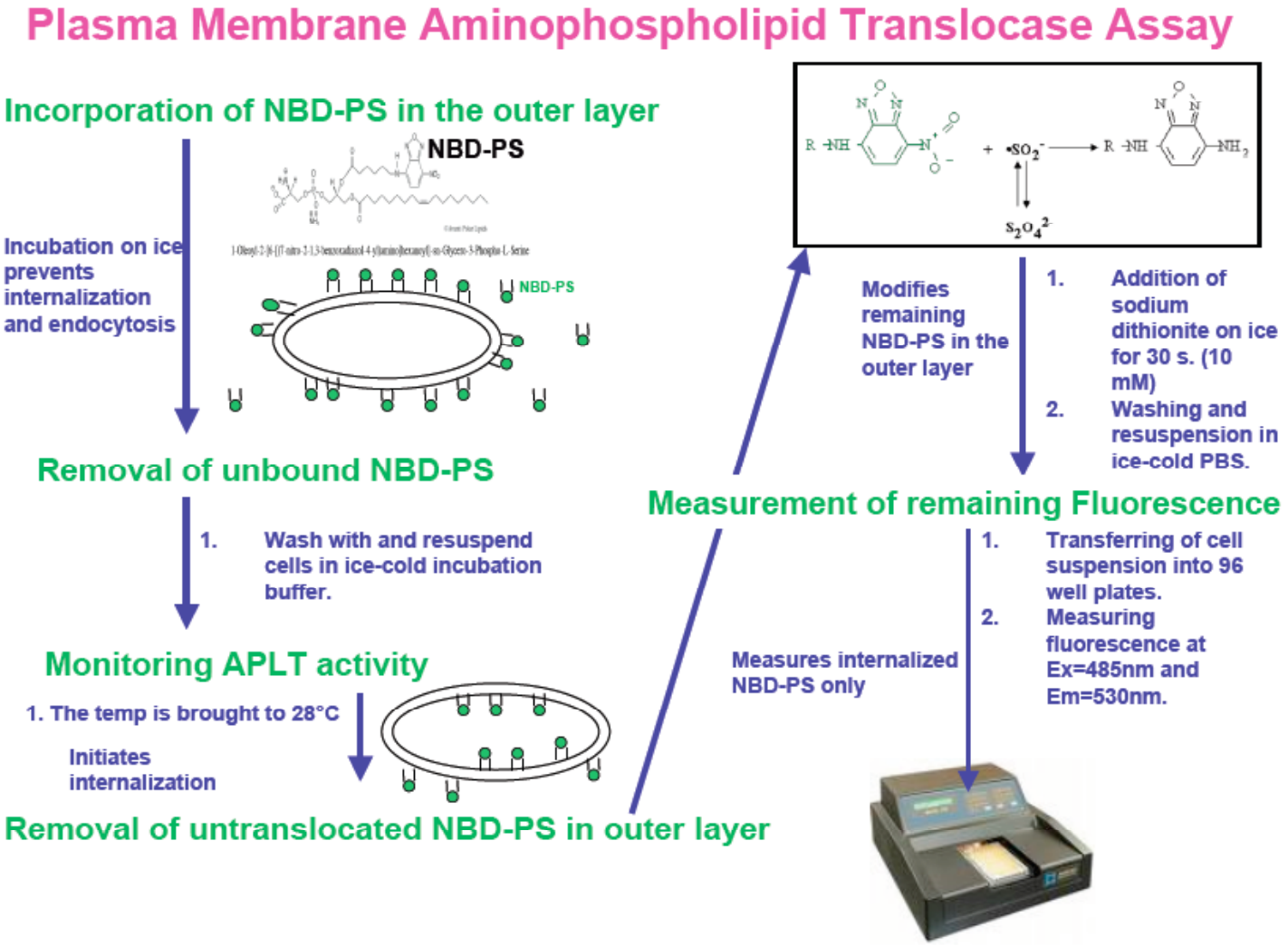

Figure 5: Our modified aminophospholipid translocase (APLT) assay.

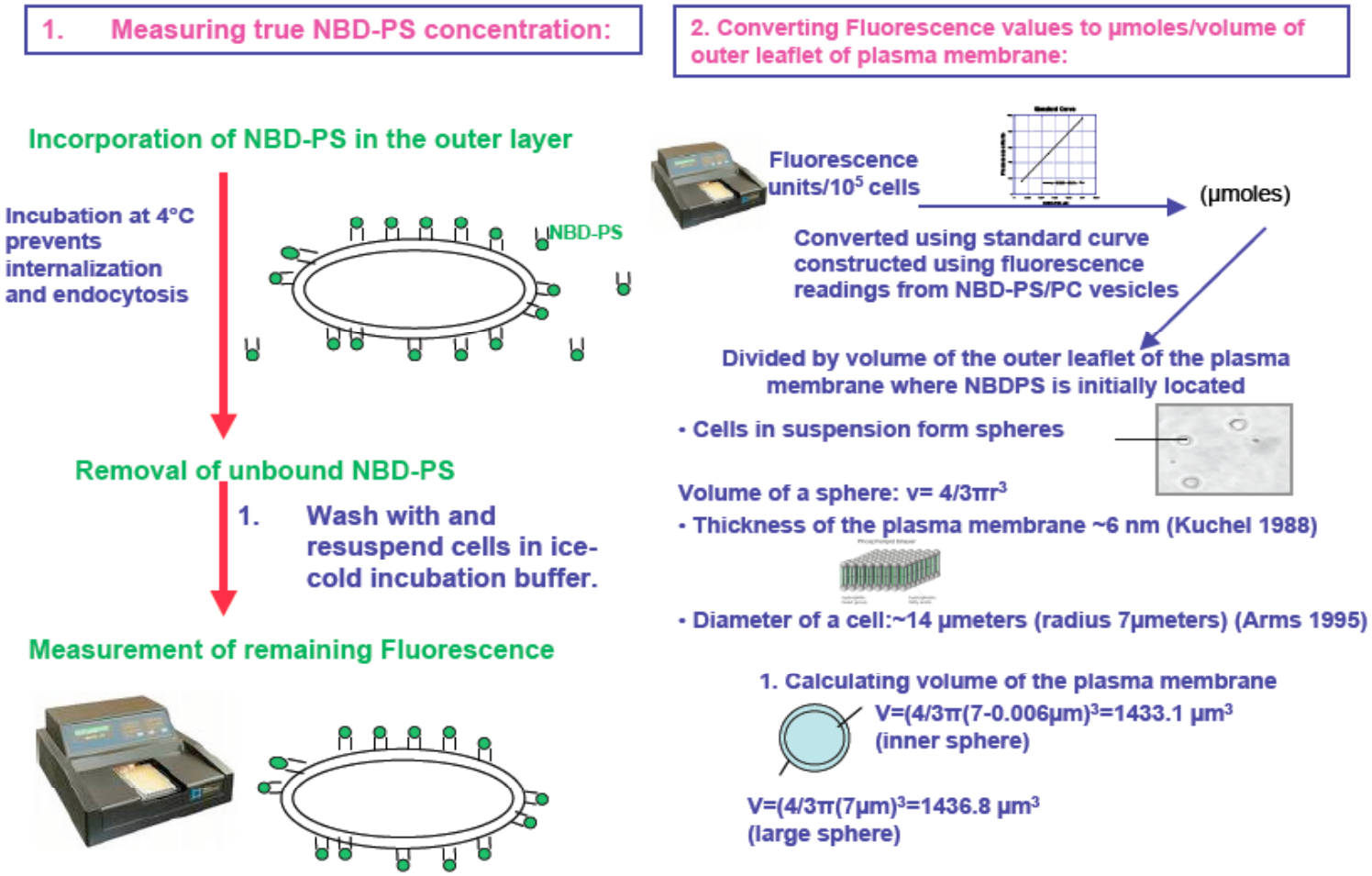

Figure 6: Calculating NBD-PS concentration incorporated into the outer leaflet of the plasma membrane. (1) Measuring true NBD-PS concentration. & (2) Conversion of the fluorescence values to µM/volume of outer leaflet of plasma membrane.

CHAPTER 3

RESULTS

3.1 NBD-phosphatidylserine translocation from the outer to inner leaflet of the plasma membrane of neuroblastoma cell line N18:

We began our study in determining the role of Atp8a1 in the plasma membrane APLT activity of neuronal cells by testing our modified APLT assay in a time-course assay performed on untransfected neuroblastoma cells (N18). In Figure 7, a time-dependent APLT assay is shown, in which by fluorescence microscopy, NBD-PS internalization is observed as incubation at 28 °C is continued (temperature at which NBD-PS translocation initiates) in the mouse neuroblastoma cell line N18. As described in materials and methods, in the APLT assay used in our studies, NBD-PS is allowed to incorporate into the outer leaflet of the plasma membrane at 4 °C for 10 min. Spontaneous incorporation of NBD-PS into suspended cells at 4 °C has been previously shown by Connor and Schroit (Connor 1989). At this temperature, aminophospholipid translocation or endocytosis, does not occur (Suzuki 1997). In order to measure only fluorescence representing NBD-PS translocated to the inner leaflet of the plasma membrane, NBD-PS fluorescence remaining in the outer leaflet (untranslocated NBD-PS) needs to be removed. In 1991, McIntyre *et al* developed a method for chemically modifying NBD to a nonfluorescent fluorophore (ABD) in both artificial and biological membrane using dithionite treatment. Figure 8 shows the reaction mechanism for the reduction of NBD-PS by dithionite. In their studies, McIntyre *et al* showed that sodium dithionite reacts only with the NBD-PS present in the outer leaflet of the plasma membrane (McIntyre 1991). Thus, in our modified APLT assay, after incubation at 28

°C, NBD-PS fluorescence remaining in the outer leaflet of the plasma membrane was removed by treating the cells with sodium dithionite. The final fluorescence observed corresponds to NBD-PS translocated by the APLT enzyme to the inner layer of the plasma membrane. An increase or decrease in fluorescence in the dithionite-treated cells corresponds to an increase or decrease in the plasma membrane APLT activity, respectively.

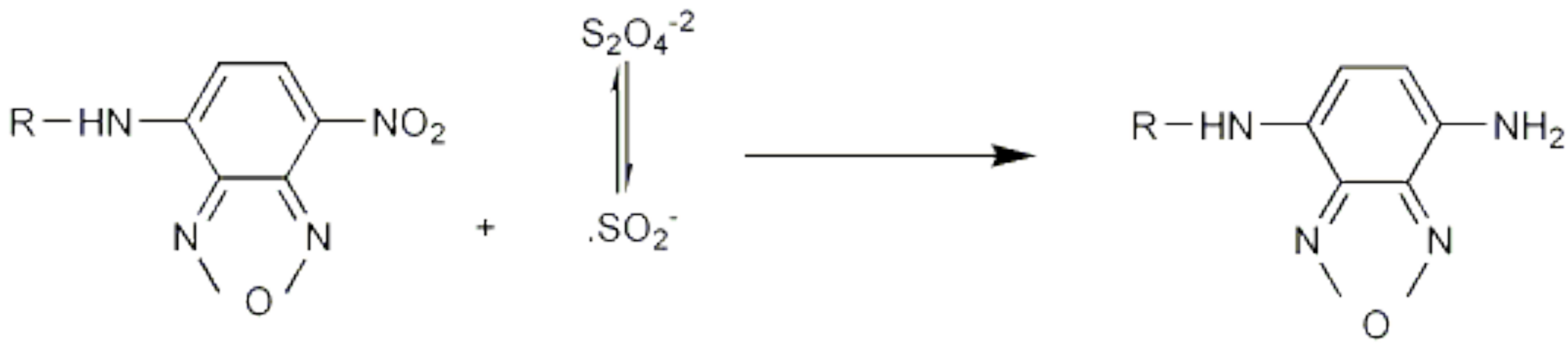

NBD-PS **Sodium Dithionite** **ABD-PS**

R Group = phosphatidylserine (1,2-dioleoyl-*sn*-glycero-3-phospho-L-serine)

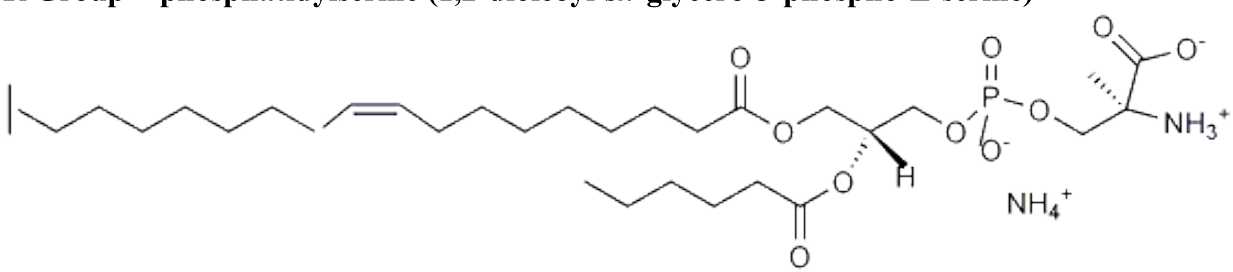

Figure 7: Reduction of NBD-PS (1-Oleoyl-2-[6-[(7-nitro-2-1,3-benzoxadiazol-4-yl)amino]hexanoyl]-sn-Glycero-3-Phospho-L-Serine) to ABD-PS 1-Oleoyl-2-[6-[(7-amino-2-1,3-benzoxadiazol-4-yl)amino]hexanoyl]-sn-Glycero-3-Phospho-L-Serine by sodium dithionite (McIntyre 1991).

Figure 8: Time-dependent translocation of NBD-PS from outer to inner leaflet of the plasma membrane of N18 cells. The N18 cells were first labeled with NBD-PS on ice for 10 min (see methods), washed free of NBD-PS, and then resuspended in an ice-cold incubation buffer, followed by incubation at 28 °C for increasing periods of time. After incubation, the cell suspension was placed back on ice. In a parallel set of samples the NBD-PS fluorescence from the outer leaflet of the membrane was removed by incubation on ice in 10 mM sodium dithionite for 30 s. The cells were then washed and resuspended in mounting fluid for fluorescence microscopy.

Kinetics of NBD-PS internalization:

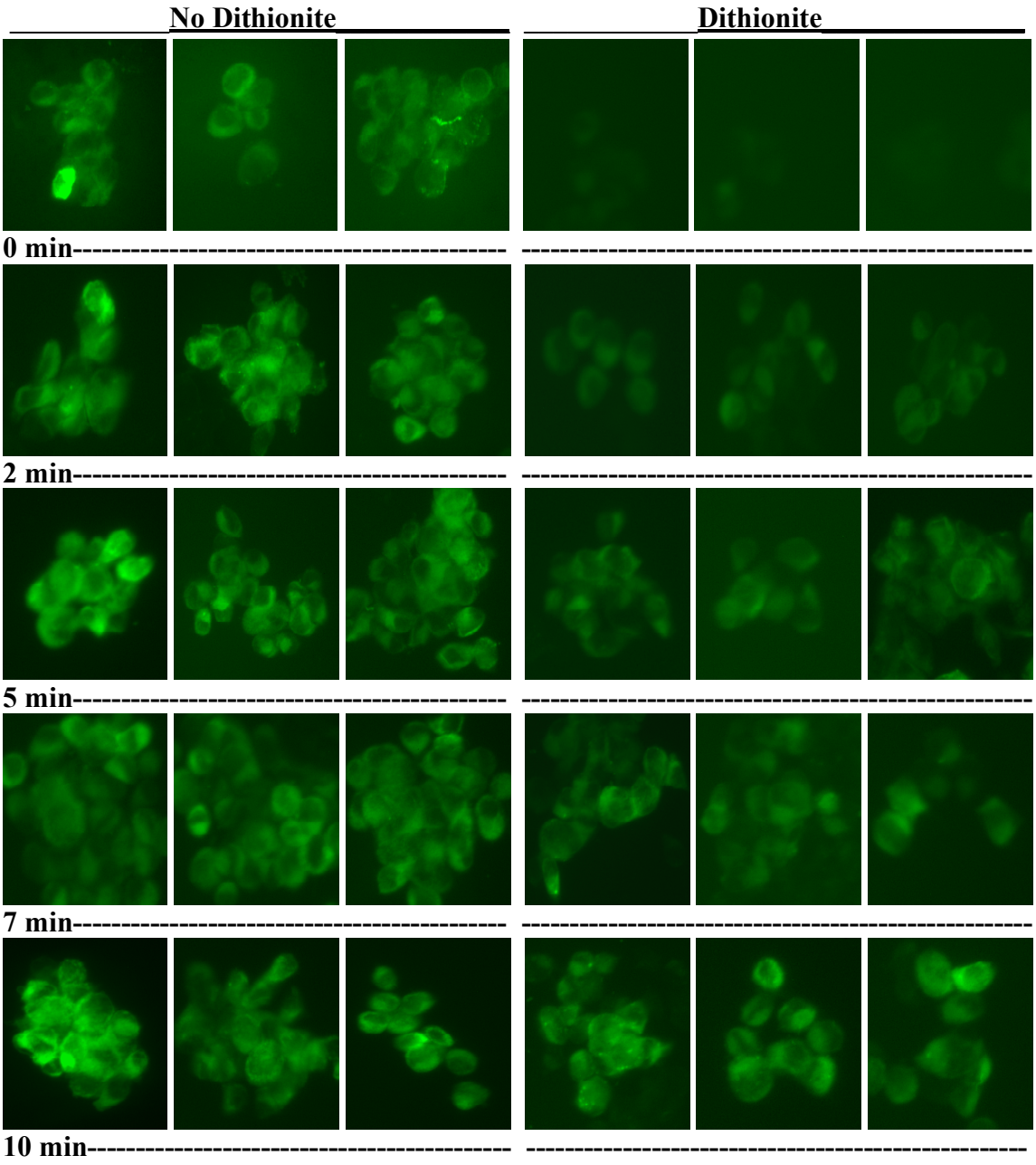

3.2 Overexpression of Atp8a1 causes an increase in the plasma membrane APLT activity of the neuroblastoma cell line N18, but not of differentiated HN2 cells:

Having tested our modified APLT assay, and obtained reproducible results in measuring the plasma membrane APLT activity, we were then ready to determine changes in the plasma membrane APLT activity due to overexpression and/or suppression of Atp8a1. As stated in materials and methods, we measured fluorescence (corresponding to translocated NBD-PS) using a microplate reader, which allowed quantitative analysis of multiple samples.

We began by overexpressing Atp8a1 in two cell lines: HN2 (hippocampal-derived cell-line) and N18. Trasient overexpression of Atp8a1 in both cell lines was confirmed by immunoblotting analysis using the Atp8a1 antibody kindly provided by Dr. Xie (Ab-B). Time-course APLT assays were used to measure the changes in APLT activity due to overexpression. The time-course was done as described in materials and methods, with incubation at 28° C up to 20 min. The data were expressed as increase in NBD-PS translocation (Atp8a1-empty vector) as percent empty vector transfeced cells.

The results obtained showed that overexpression of Atp8a1 in N18 cells caused an increase in APLT activity (increase in NBD-PS fluorescence). However, when overexpressed in HN2 cells, Atp8a1 caused a decrease in APLT activity (Figure 9), possibly due to non-specific inhibition of the endogenous PM-APLT protein, which was therefore not Atp8a1.

These results led us to hypothesize that Atp8a1 could be the plasma membrane APLT enzyme in N18 cells, but not in HN2. Although expression of Atp8a1 in HN2 cells was similar to that in N18 cells, Atp8a1 was not the main PM-APLT enzyme in these

cells. Thus the PM- APLT activity of Atp8a1 could be cell-type specific. A different homolog (e.g. Atp8a2, Atp8a1 closest homolog) could be functioning as the PM-APLT in the non-tumorigenic cell-line, HN2.

Figure 9: Overexpression of Atp8a1 causes an increase in the plasma membrane APLT of N18 cells, but not of HN2. N18 and differentiated HN2 cells overexpressing Atp8a1 were harvested and subjected to time-course APLT assays as described in the materials and methods. (a) and (b) Overexpression of Atp8a1 in both N18 and HN2 cells was confirmed by immunoblotting using ab-B. (c) and (d) The time-course APLT assays show an increase in NBD-PS translocation in transfected N18 cells but not in transfected HN2.

Atp8a1 Overexpression in N18 and HN2 cells

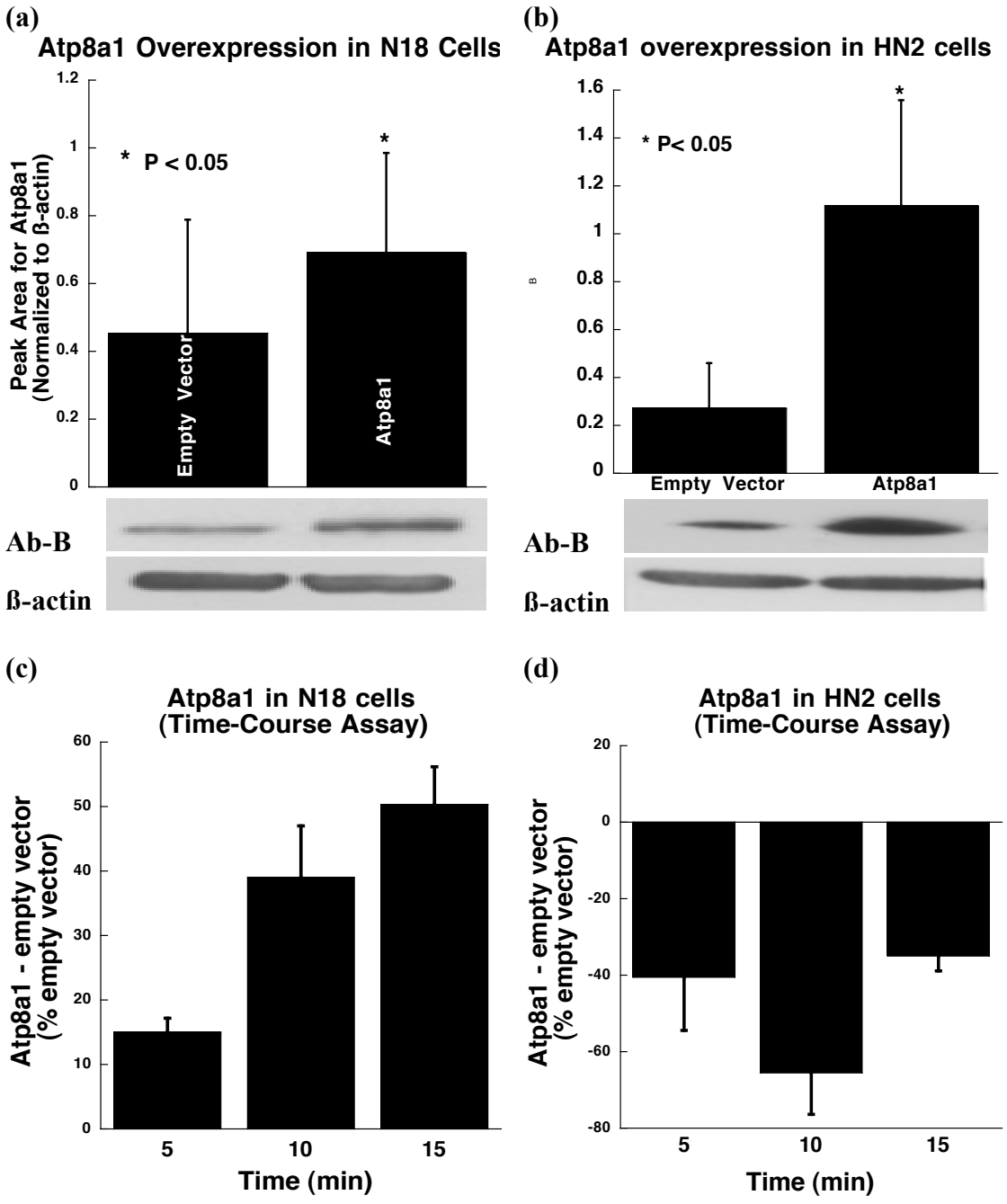

3.3 Transient overexpression of Atp8a1 in N18 cells causes an increase in Vmax and no change in Km for the plasma membrane APLT:

As stated above, overexpression of Atp8a1 in N18 cells causes an increase in NBD-PS translocation from the outer to the inner leaflet of the plasma membrane, an increase in the plasma membrane APLT activity. Thus, Atp8a1 could be the plasma membrane APLT in N18 cells. To further test this hypothesis, we approached this question through kinetic analysis, by measuring the Km and Vmax values using our modified APLT assay.

Vmax and Km are the two parameters that define the kinetic behavior of an enzyme as a function of its substrate concentration. As stated in the Michaelis-Menten equation for a unimolecular reaction, a particular enzyme catalyzing the conversion of a specific substrate at a definite temperature and pH, displays one definite Km value. Thus, if a different enzyme molecule catalyzes the same reaction, its affinity for the substrate will be different, which will be reflected in a new Km value for this enzyme. Vmax is also a characteristic feature for the enzyme. If the Km value remains the same, then any change in Vmax value would reflect a change in the number of molecules of the enzyme. If Atp8a1 were indeed the plasma membrane APLT enzyme in N18 cells, then overexpression of this molecule would cause an increase in the Vmax value due to an increase in the number of APLT molecules catalyzing the translocation of NBD-PS. This was exactly what our results showed when Atp8a1 was transiently overexpressed in N18 cells.

To determine changes in Km and Vmax values, substrate concentration-dependant PM-APLT assays were conducted. As described in materials and methods, different concentrations of NBD-PS were used (0, 0.035, 0.5, 0.75, 1, 2 μM). The incubation time at 28 °C, which initiates translocation of NBD-PS, was maintained for 10 min (as shown in Figure 9, the APLT activity remains in the linear range up to 10 min). To correctly report the true Km values for the PM-APLT enzyme, the concentration of NBD-PS incorporated to the outer layer of the plasma membrane (before internalization) was determined. Briefly as described in materials and methods, parallel samples were used and cells were allowed to incorporate NBD-PS on ice for 10 min. After this, any unbound NBD-PS was removed and the fluorescence remaining was measured and converted to micromolar concentrations of NBD-PS by comparing with a standard curve constructed using fluorescence readings from NBD-PS/PC vesicles. Values were further converted to μmoles/min/cell and divided by the volume of the plasma membrane, which was calculated as shown in Figure 6. In this experiment, overexpression of Atp8a1 in N18 cells was confirmed by immunocytochemistry using a *Myc*-ab (as stated in Materials and Methods, cDNAs for Atp8a1 and Atp8a2 were cloned into the expression vector pcDNA6.1/*myc*-His in-framed with epitope tags) (Figure 10a). Substrate concentration-dependant curves were obtained by plotting fluorescence units/10^5 cells (NBD-PS translocation from outer to inner leaflet) versus NBD-PS concentration (in μM) (Figure 10 (b)). Km and Vmax values were calculated by graphing a Lineweaver-Burk plot (produced by plotting the inverse of substrate concentration against the inverse of the fluorescence units/10^5 cells). The Lineweaver-Burk plots for this experiment are shown

in Figure 10 (c) and (d). Table 2 summarizes results obtained from three separate substrate saturation APLT assays, each with triplicate samples.

As expected, the results obtained show that overexpression of Atp8a1 in the N18 cells causes no change in the Km value of the endogeneous PM-APLT that catalyzes the translocation of NBD-PS from the outer to the inner leaflet of the plasma membrane. There was a significantly 1.7-fold increase (paired t-test) in the Vmax value of this enzyme in the Atp8a1 overexpressing cells. This strongly suggests that Atp8a1 is the plasma membrane APLT of the N18 cells (the same Km value) and that the process of transfection causes an overall increase in the number of APLT molecules in these cells (increase in Vmax value of APLT).

Figure 10: Transient overexpression of Atp8a1 in the mouse neuroblastoma cell line N18 causes an increase in Vmax without any change in Km. (a) The Atp8a1-pcDNA6/*myc*-His transfected N18 cells showed immunostaining with a Myc Ab. (b) Substrate saturation curves show a Atp8a1-mediated increase in Vmax. (c) and (d) Lineweaver-Burk analysis reveals that overexpression of Atp8a1 in N18 cells elicits an increase in Vmax without affecting the Km value.

Plasma membrane APLT kinetics in N18 cells overexpressing Atp8a1

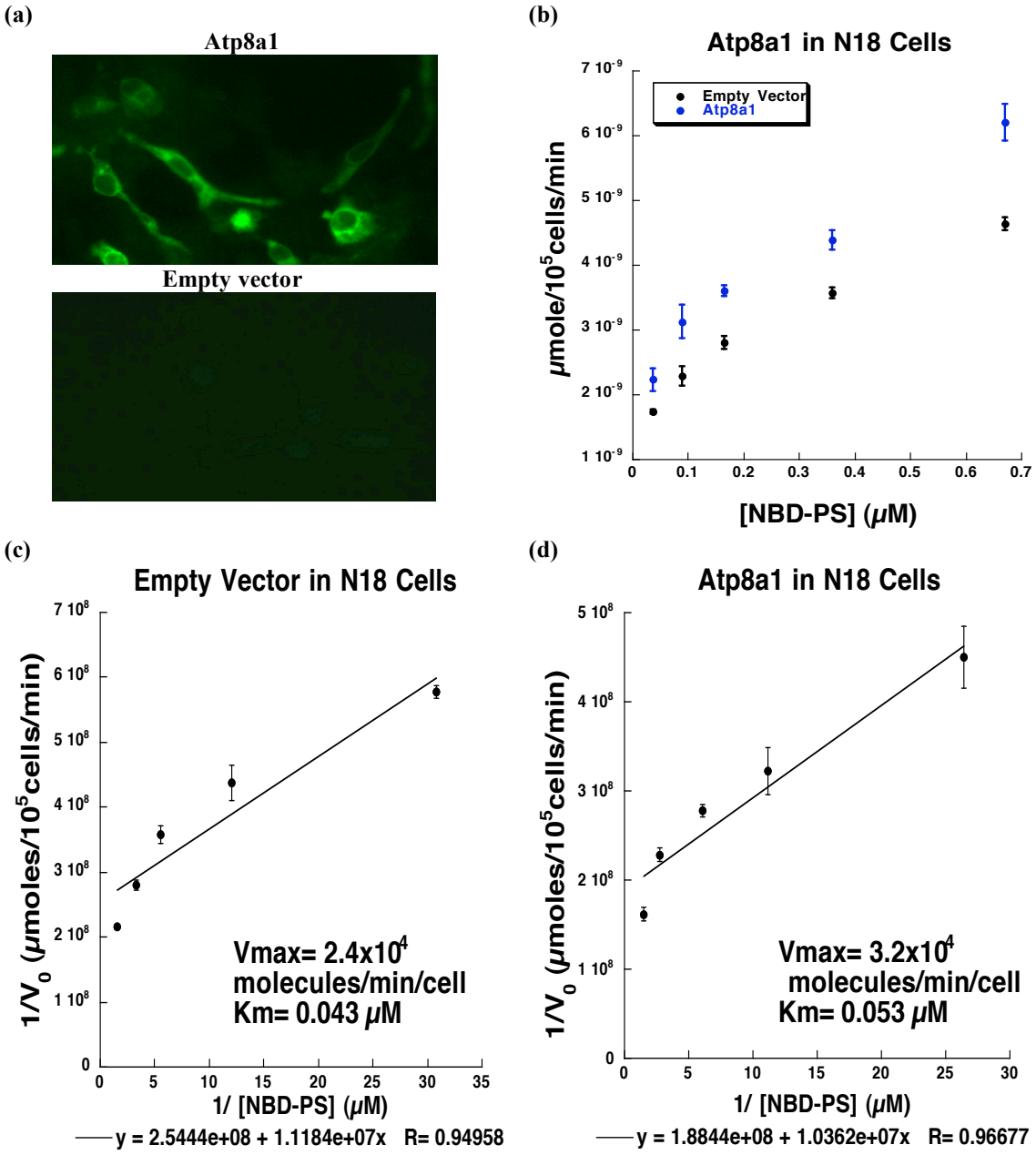

Table 2: Atp8a1 overexpression causes an increase in Vmax value of the APLT activity of the plasma membrane of N18 cells.								
Exp.	**Empty Vector in N18**			**Atp8a1 in N18**			**Fold Increase in Vmax in presence of Atp8a1**	
	K_m (µM)	**K_m(µM) Mean± Std.Dev.**	**V_{max} (molecules/ min/cell)**	**K_m (µM)**	**K_m(µM) Mean± Std.Dev.**	**V_{max} (molecules/ min/cell)**	**Fold Increase**	**Mean± Std.Dev**
1	**0.033**		**0.76×10^4**	**0.029**		**1.1×10^4**	**1.45**	
2	**0.011**	**0.029±0.02**	**0.73×10^4**	**0.028**	**0.037±0.01**	**1.5×10^4**	**2.1**	**1.7±0.37**
3	**0.043**		**2.6×10^4**	**0.053**	**P=0.3402**	**3.2×10^4**	**1.3**	**P=0.0449**

(Paired t-test was used for data analysis because, in each experiment, aliquots of the same batch of cells were transfected with the two vectors)

3.4 Transient expression of Atp8a1 phosphorylation-site mutants in N18 cells causes a decrease in the Vmax value without affecting the Km value for the plasma membrane APLT:

To confirm our hypothesis that Atp8a1 is the plasma membrane APLT of N18 cells, we examined the effect of suppressing At8a1 activity on the translocation of NBD-PS in these cells.

In order to suppress the activity of Atp8a1, we created phosphorylation site mutants. As stated previously, Atp8a1 is a P-type ATPase. All P-type ATPases are composed of four principal domains: the phosphorylation, the ATP-binding, the amino-terminal and the membrane domain (lipid- binding site in Type IV P-type ATPase) (Kuhlbrandt 2004). Thus, phosphorylation, ATP binding and phospholipid binding occur in separate domains. The ATPase activity of P-type ATPases depends on the phosphorylation of the aspartic residue at the beginning of the P-type signature domain: **D**KTGT[L,I,V,M][T,I,S], which is at position D409 in Atp8a1. To eliminate phosphorylation of this protein and, thereby, its ATPase activity, without affecting both ATP and PS binding (which occur in separate domains), we mutated the aspartic acid residue to a lysine residue. This non-conservative mutation allows binding of ATP and PS, but it prevents both hydrolysis of ATP and PS translocation. Thus, such mutants could function as a dominant negative versions of the target protein. Dominant negative mutation, first described by Herskowitz in 1987, is a tool used to study the function of specific genes. These mutants which compete with the wild-type enzyme for its substrate, can "efficiently inhibit any functional consequence of the wild-type enzymatic activity," if the enzymatic reaction is limited by the substrate concentration (Sheppard 1994). Thus,

our Atp8a1 phosphorylation site mutants could be potential dominant negative mutants that could compete for PS binding. Alternatively, in the presence of excess substrate, they could compete with the binding of Atp8a1 to a chaperone that assists the protein in being targeted to in the plasma membrane. Therefore, they could suppress Atp8a1 activity in the cells.

The site-directed mutagenesis was performed as described in Materials and Methods. Two Atp8a1 mutants were created: D409K and D409E. For the kinetic analysis, the Atp8a1-D409K mutant was used to suppress the activity of Atp8a1. Supporting our hypothesis, the results (Figure 11 and Table 3) showed a significant (0.5-fold) decrease in the Vmax value of the APLT enzyme without any significant change in the Km value. Like other experiments, these were repeated three times for statistical analysis.

Figure 11: Transient expression of the Atp8a1-D409K phosphorylation site mutant causes an inhibition of Vmax without any significant change in Km for the APLT activity in the N18 cells. (a) The Atp8a1-D409K-pcDNA6/*myc*-His transfected N18 cells showed immunostaining with a Myc Ab. (c) and (d) Lineweaver-Burk analysis showed that expression of Atp8a1-D409K in N18 cells elicits a decrease in Vmax without affecting the Km value for plasma membrane APLT.

Plasma membrane APLT kinetics in N18 cells expressing Atp8a1-D409K

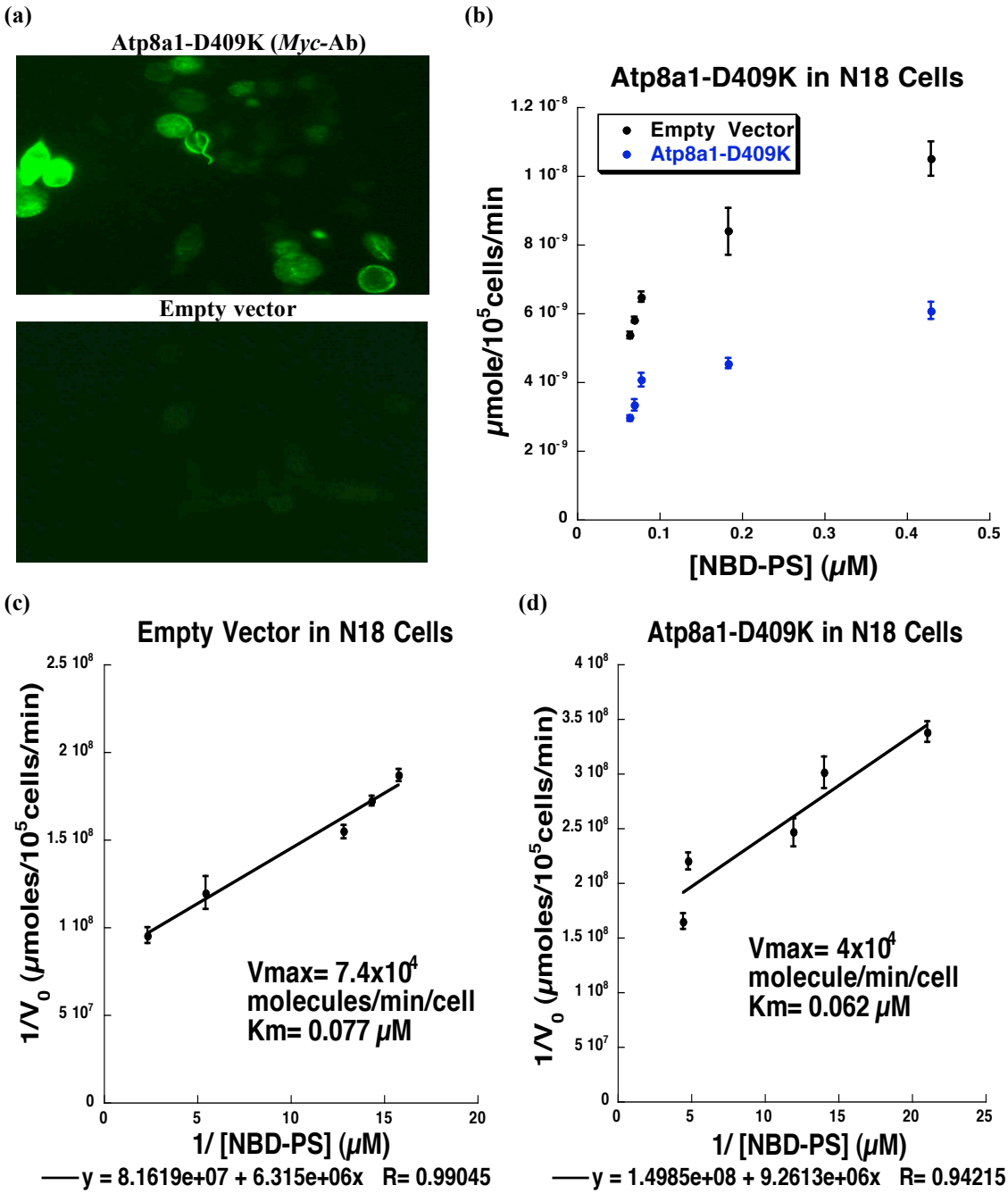

Table 3: Atp8a1-D409K expression causes a decrease in Vmax value of the APLT activity of the plasma membrane of N18 cells.								
Exp.	Empty Vector in N18			Atp8a1-D409K in N18			Fold Increase in Vmax in presence of Atp8a1-D409K	
	K_m (µM)	K_m(µM) Mean± Std.Dev.	V_{max} (molecules/ min/cell)	K_m (µM)	K_m(µM) Mean± Std.Dev.	V_{max} (molecules/ min/cell)	Fold Increase	Mean± Std.Dev
1	0.077		$6.3x10^4$	0.062		$3.2x10^4$	0.508	
2	0.089	0.105±0.04	$7.4x10^4$	0.085	0.074±0.012	$4x10^4$	0.581	0.55±0.037
3	0.150		$3.6x10^4$	0.074	P=0.2929	$2.0x10^4$	0.556	P=0.0351

(Paired t-test was used for data analysis because, in each experiment, aliquots of the same batch of cells were transfected with the two vectors)

3.5 Expression of phosphorylation site mutants of Atp8a1 in N18 cells leads to PS externalization:

To further establish that Atp8a1 is the plasma membrane APLT in N18 cells, maintaining the asymmetric distribution of phosphatisylserine, we assayed PS externalization. If Atp8a1 is the PM-APLT of N18 cells, then suppression of its activity by overexpression of phosphorylation site mutants should lead to an increase in PS externalization.

In this study, N18 cells were transiently transfected with vectors expressing Atp8a1 mutants and analyzed by the standard surface-labeling assay using Alexafluor488-coupled annexin V (annexin V binds specifically to externalized PS). The results showed that expression of the Atp8a1 mutants, but not sense Atp8a1 or the empty vector, caused pronounced PS externalization in these cells. Transfection efficiency was confirmed by co-transfection with a pAsRed2-N1vector, which expresses the red fluorescent protein AsRed2, and the number of PS-exposed cells was normalized to the number of transfected cells for quantification and statistical analysis (Figure 12).

Figure 12: Transient expression of Atp8a1 mutants causes externalization of PS in the N18 cells. (a) Transfection of the mutants of Atp8a1 causes PS externalization as shown by staining with annexin V-Alexafluor488 (Green) (Annexin V binds to PS). Co-transfection of the pAsRed2-N1 vector (Red) differentiates the transfected cells from the non-transfected. Pictures shown are representative of two experiments, each performed with triplicate wells of N18 cells. (b) Enlarged pictures show outer leaflet plasma membrane annexin staining in the mutant Atp8a1-expressing cells as compared to empty vector-transfected or sense, wild type Atp8a1-expressing cells. (c) The number of annexin V-stained cells was normalized to the total number of transfected cells/well and the values used for statistical analysis using paired t-test.

(a) **Expression of Atp8a1 phosphorylation site-mutants leads to PS externalization**

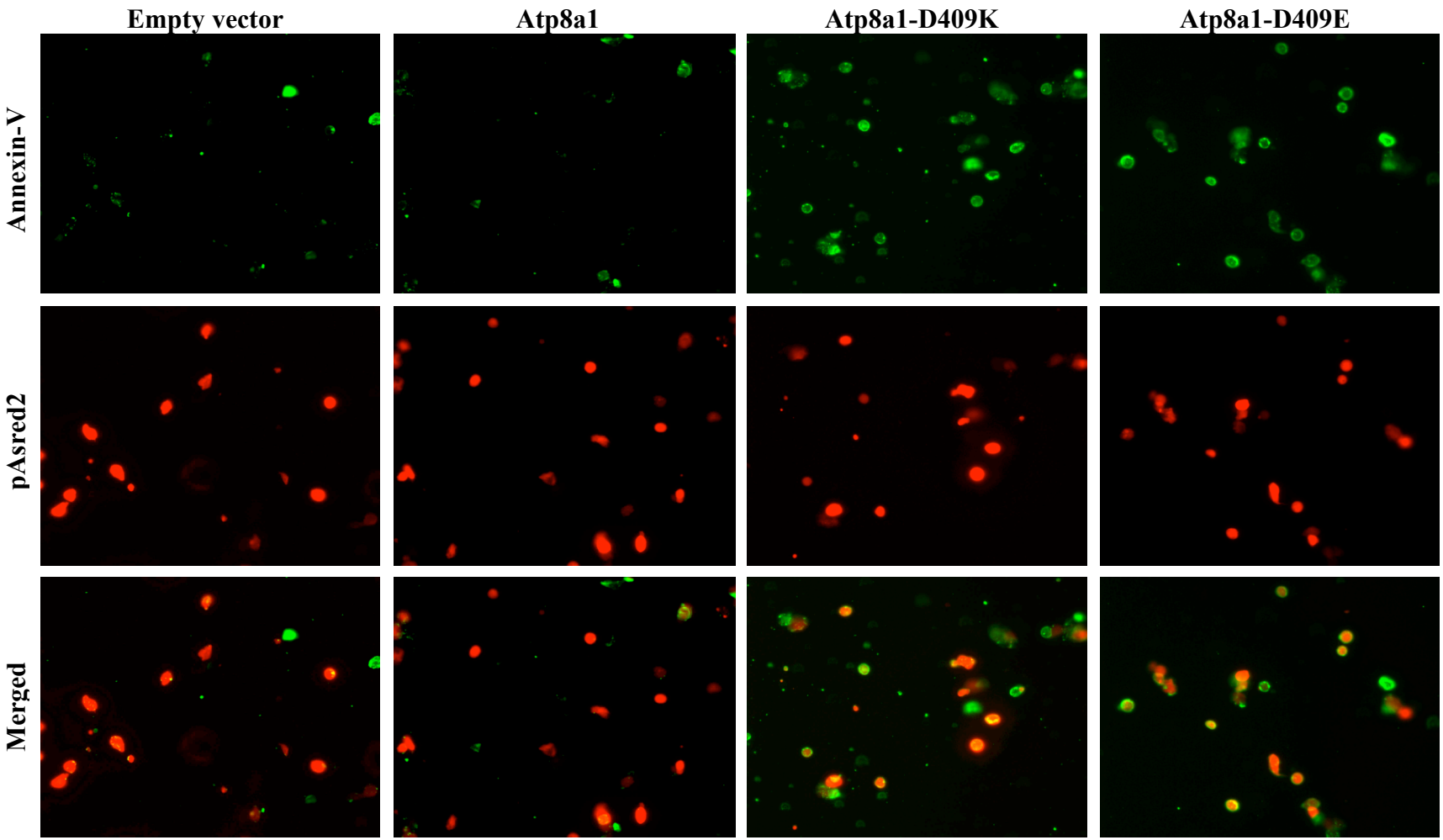

Figure 12: (continued)

(b)

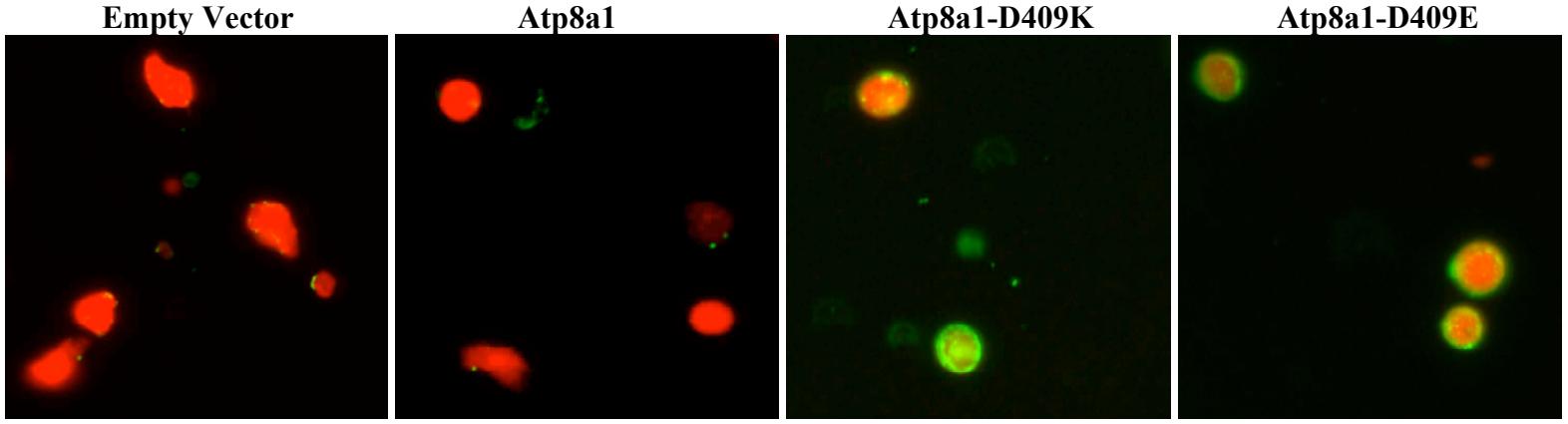

(c)

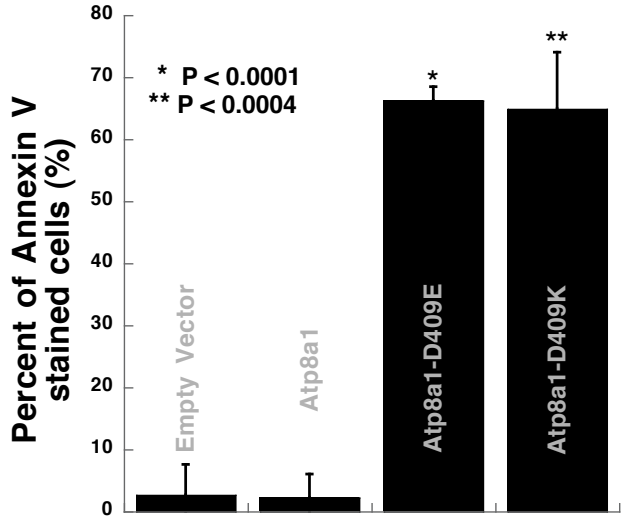

3.6 Transient overexpression of Atp8a2 causes a decrease in both Km and Vmax values of the plasma membrane APLT in the mouse neuroblastoma cell line N18:

So far, our data indicates that Atp8a1 is the plasma membrane APLT in N18 cells. However, to demonstrate that these changes observed were not an artifact of transfection that would result from expression of any Type-IV P-type ATPase, we transiently overexpressed Atp8a2 and determined the Km and Vmax values. Overexpression of Atp8a2 in N18 cells was confirmed by western blot analysis using the Atp8a2 antibody (ATPase IB ab) and by immunocytochemistry using a Myc-antibody. In contrast to our previous observations with Atp8a1, overexpression of Atp8a2 caused a decrease in both Vmax and Km values (Figure 13). These results confirmed that indeed overexpression of Atp8a1 in N18 cells produces a specific increase in the plasma membrane NBD-PS translocation. The decreased observed in the presence of overexpressed Atp8a2 could be due to a non-specific effect exerted by this molecule on the endogenous plasma membrane APLT.

Figure 13: Unlike Atp8a1, Atp8a2, causes a decrease in Vmax and Km for NBD-PS translocation in N18 cells. (a) Immunoblotting using an Atp8a2 antibody shows a significant increase in Atp8a2 expression in Atp8a2-pcDNA6.1/*myc*-His C transfected cells (paired t-test, n=3). (b) The Atp8a2-pcDNA6.1/*myc*-His-transfected N18 cells showed immunostaining with a Myc Ab, but the empty vector-transfected cells showed no staining. (c) The substrate saturation curves indicate no increase in Vmax in the Atp8a2 overexpressing cells. (d) & (e) Lineweaver-Burk analysis showed that overexpression of Atp8a2 in N18 cells changes both Vmax and Km.

Plasma membrane APLT kinetics in N18 cells overexpressing Atp8a2

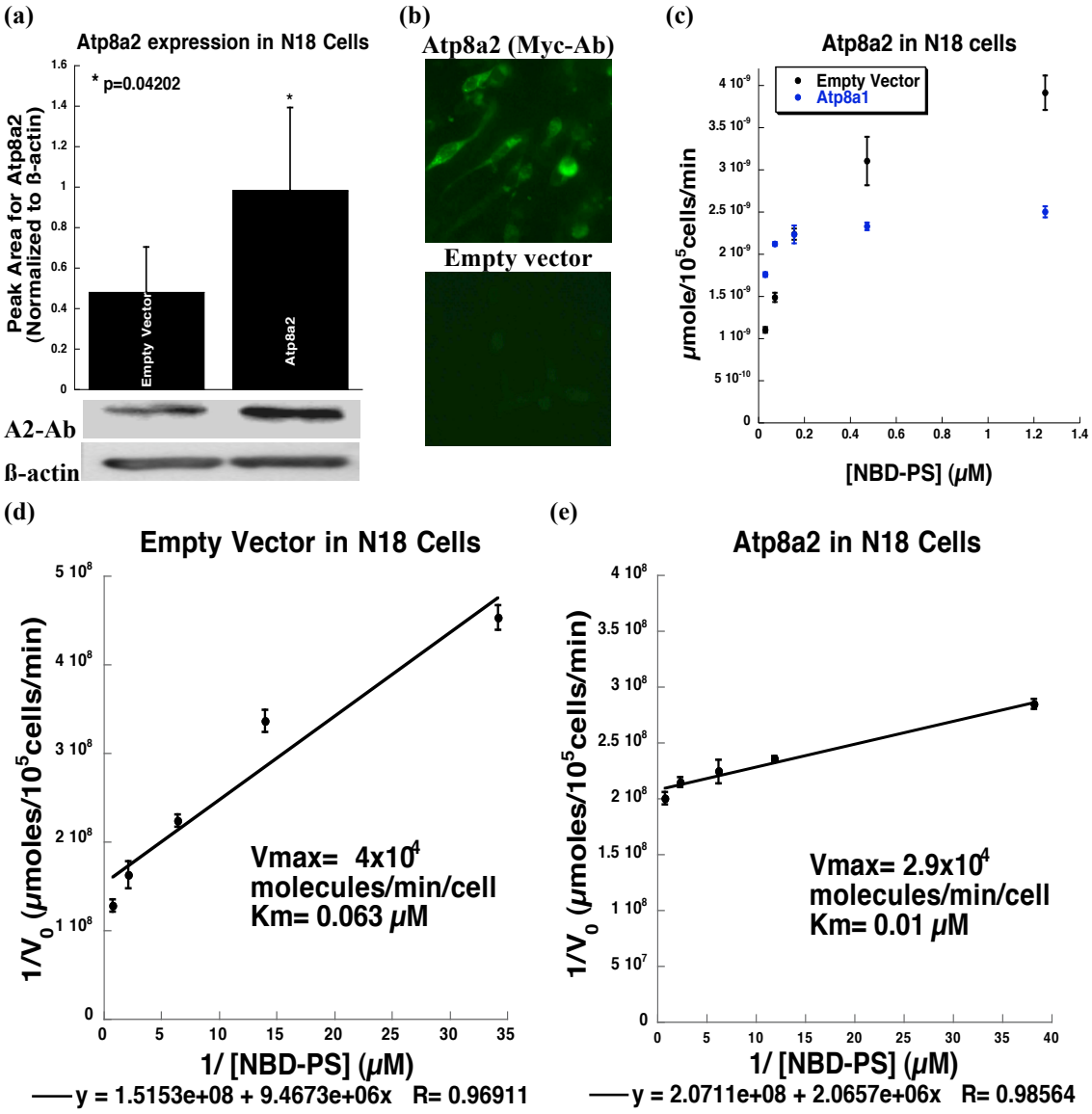

Table 4: Atp8a2 overexpression causes a decrease in Vmax value of the APLT activity of the plasma membrane of N18 cells.								
Exp.	**Empty Vector in N18**			**Atp8a2 in N18**			**Fold Increase in Vmax in presence of Atp8a2**	
	K_m (µM)	**K_m(µM) Mean± Std.Dev.**	**V_{max} (molecules/ min/cell)**	**K_m (µM)**	**K_m(µM) Mean± Std.Dev.**	**V_{max} (molecules/ min/cell)**	**Fold Increase**	**Mean± Std.Dev**
1	**0.041**		**$6.3x10^4$**	**0.007**		**$3.2x10^4$**	**0.508**	
2	**0.063**	**0.045±0.02**	**$4.0x10^4$**	**0.01**	**0.01±0.005**	**$2.9x10^4$**	**0.725**	**0.58±0.12**
3	**0.032**		**$8.4x10^4$**	**0.016**	**P=0.08464**	**$4.3x10^4$**	**0.512**	**P=0.0884**

(Paired t-test was used for data analysis)

3.7 PS externalization in the Dentate Gyrus of Atp8a1 (-/-) mice:

We have shown that Atp8a1 is the plasma membrane APLT in the mouse neuroblastoma cell-line N18, and that its suppression leads to an increase in PS externalization. However, to better understand the physiological importance of Atp8a1 and the consequence of its elimination in neuronal cells, deletion of the gene for Atp8a1 in mice was needed. An Atp8a1 (-/-) mouse line has been prepared and characterized by Deltagen, Inc. For our studies, we obtained the Atp8a1 (+/-) mice commercially from JAX lab and paired them to obtain the Atp8a1 (-/-) mice. Genotyping of these mice was performed as described in materials and methods. As reported by Deltagen, the Atp8a1 (-/-) mice have no abnormal phenotypic characteristics.

We wanted to test a hypothesis that came into view after confirming that Atp8a1 was the plasma membrane APLT in the neuroblastoma cell line, but not in the differentiated hippocampal derived cell line. We hypothesized that Atp8a1 could be the plasma membrane APLT of fast dividing neuronal cells. As it is known, the dentate gyrus (DG) is one of the few regions of the adult brain where neurogenesis takes place. Neurogenesis has been shown to play an important role in the formation of new memories (Kee 2007). Thus, we examined PS externalization by annexin V staining in dissociated cells from the DG and hippocampal culture slices of Atp8a1 (-/-) and wild type mice. The results showed a striking increase in PS externalization in the Atp8a1 (-/-) mice over that in the wild type mice (Figure 14 and 15), thus confirming our hypothesis.

As stated above, the DG plays an important role in memory formation. Also, elimination of Atp8a1 expression leading to PS externalization in the proliferating cells of the DG may result in phagocytosis of the PS-exposed neuronal cells, as previously

observed in *C. elegans* germ cells (Darland-Ransom 2008a). Even during late embryogenesis, many proliferating neural cells present in the hippocampus of the Atp8a1 (-/-) mice may be eliminated by phagocytosis. Thus, we expected a loss of hippocampal neurons, which may contribute to behavioral deficits. The Atp8a1 (-/-) mice were subjected to behavioral analysis by using the water T-maze, which is currently used to evaluate learning and memory abilities in knockout mice. The results obtained indicated that the Atp8a1 (-/-) mice suffer from delayed hippocampal learning as compared to the wild type mice (Figure 16).

Figure 14: PS-externalization in cells from the dentate gyrus of Atp8a1 (-/-) mice but not wild type mice. (a) Cells from the DG were isolated from hippocampal slices of control and Atp8a1 (-/-) mice. Briefly, the DG was isolated using a 1.5-mm bore tissue puncher. Cells were gently dissociated and treated with Alexafluor 488-annexin V to monitor externalized PS, followed by propidium iodide (PI) treatment to detect apoptosis. (b) Enlarged pictures showing strongly stained annexin V (+) cells in the Atp8a1 (-/-) mice as compared to the wild type mice. (c) Annexin V stained cells (green) co-localized with Hoechst stained cells (Blue). (d) The number of annexin V stained cells was normalized to the total number of cells from two different mice and the values used for statistical analysis unpaired t-test.

PS externalization in dissociated cells from the DG of Atp8a1 (-/-) mice

(a)

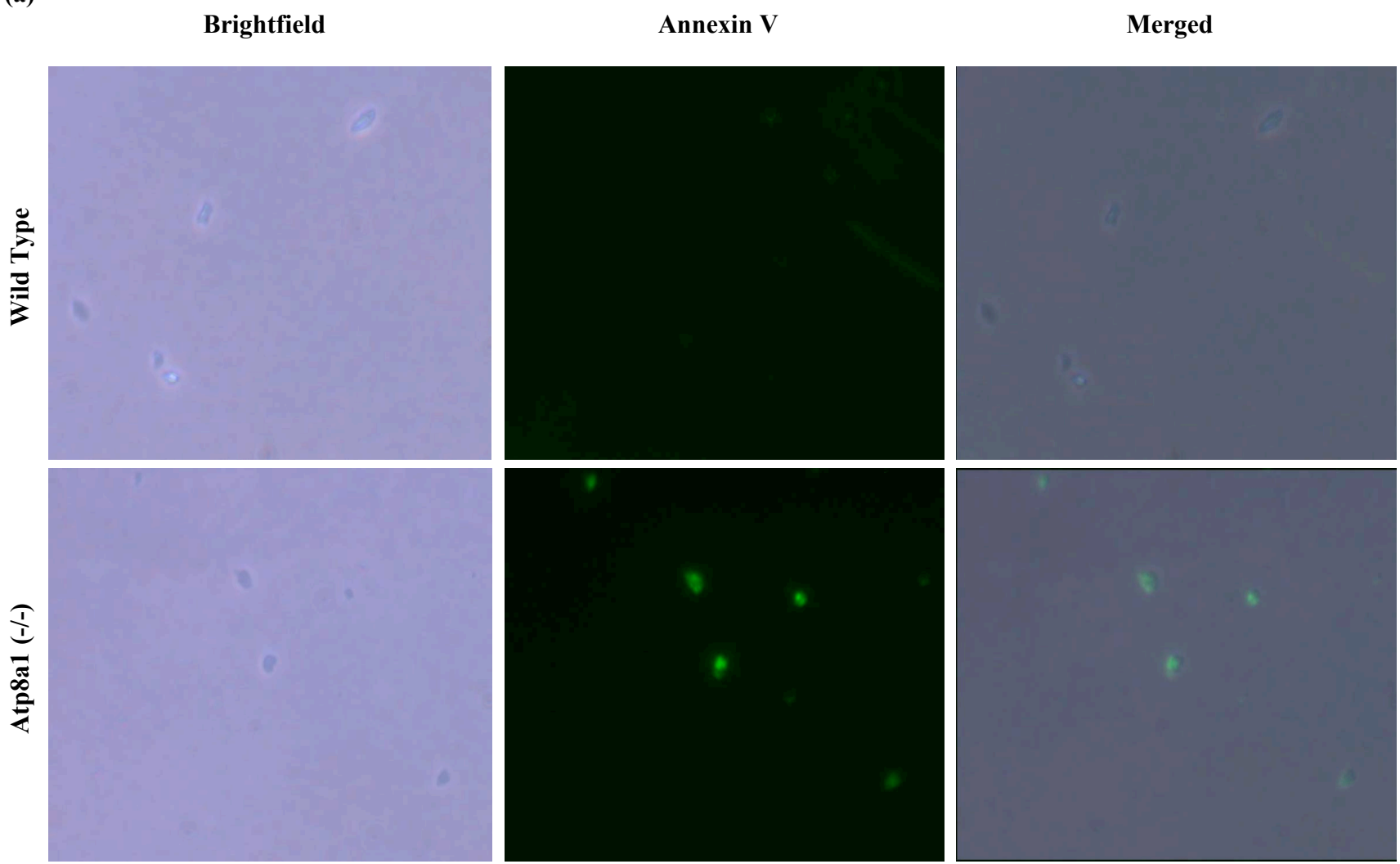

Figure 14: (Continued)

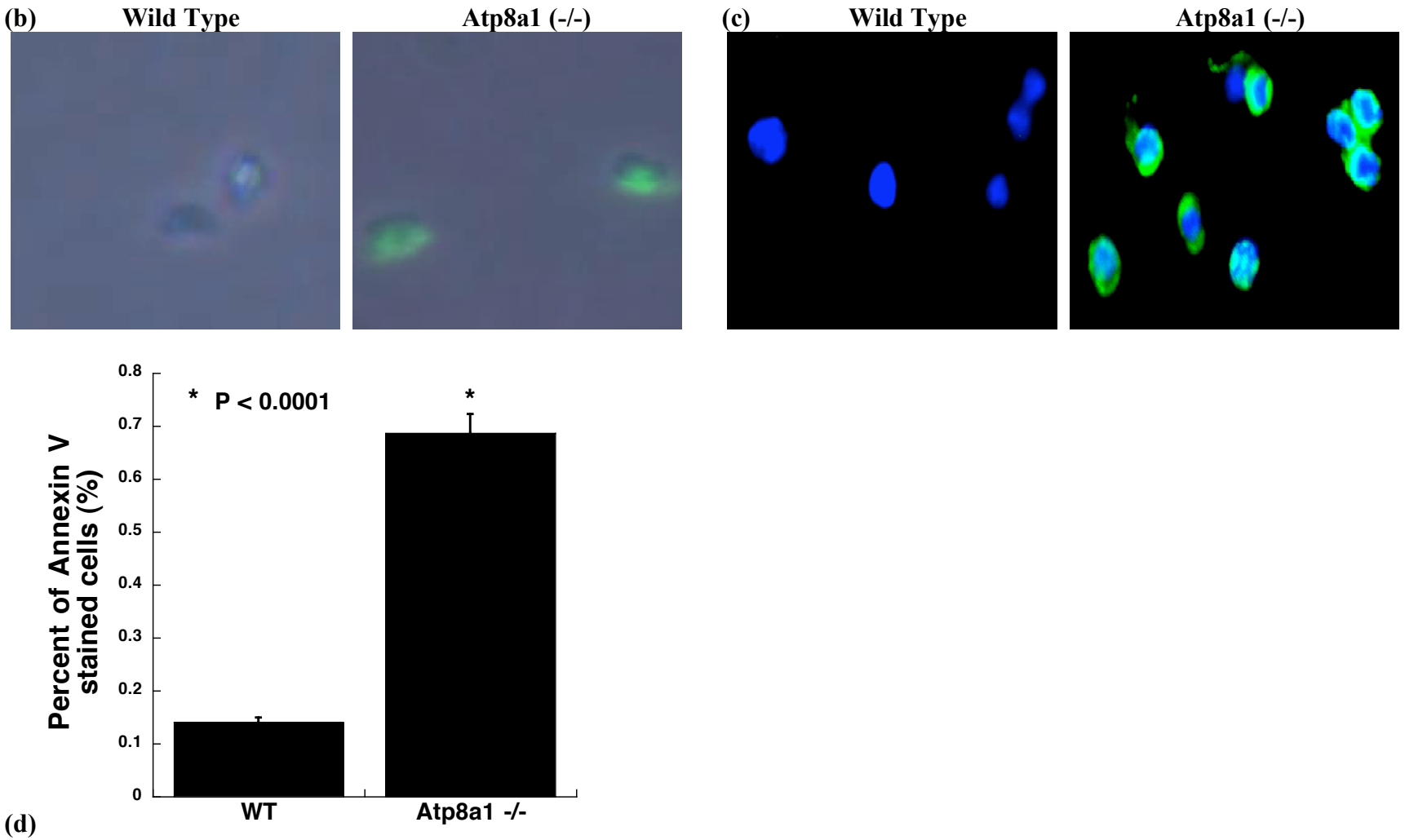

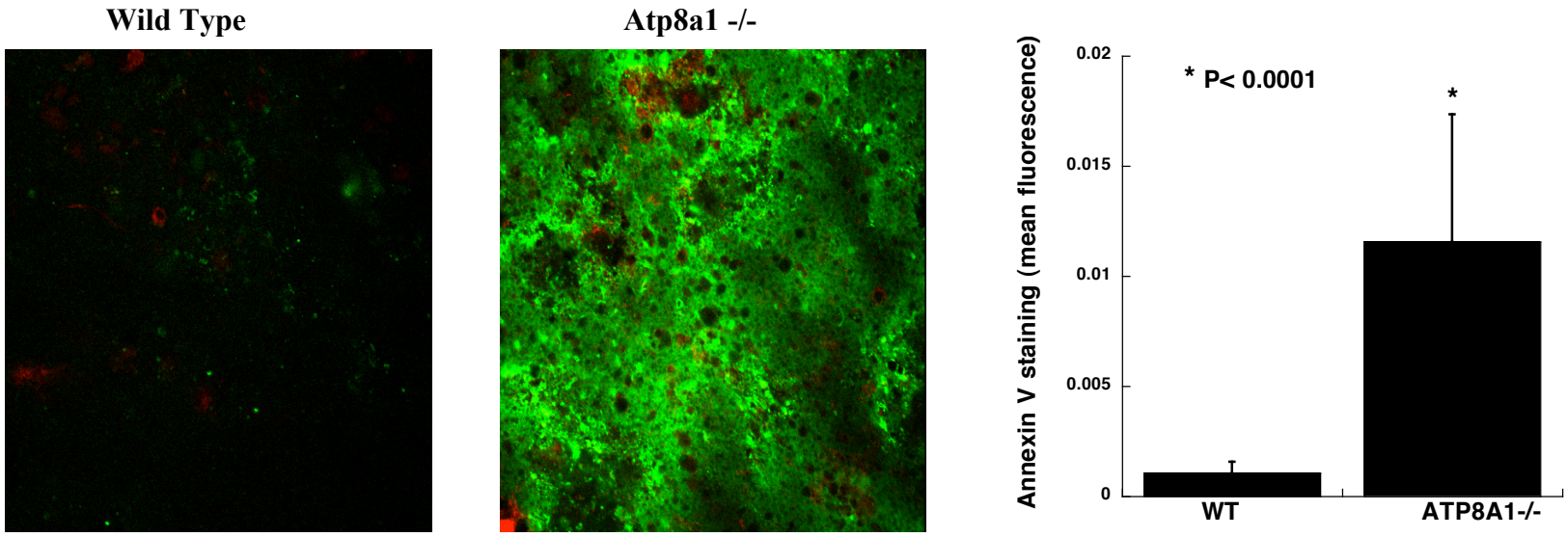

Figure 15: PS externalization observed in the DG of the Atp8a1 (-/-) mice, but not the wild type mice. Cultured hippocampal slices (400 µm) were treated with Alexafluor 488-annexin V to monitor externalized PS, followed by propidium iodide (PI) treatment to detect apoptosis. (a) Images (100x) were obtained by confocal microscopy. (b) Statistical analysis was performed using "Image J"-scans of all data from two experiments.

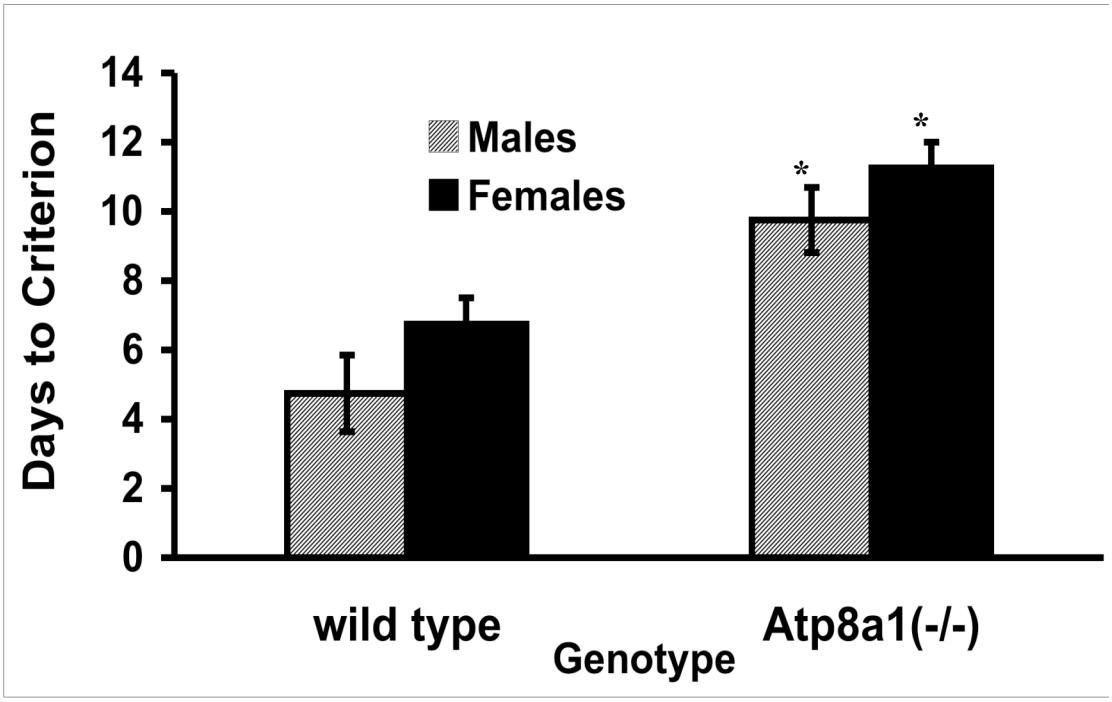

Figure 16: Atp8a1 (-/-) mice display a marked delay in hippocampal-dependent learning. The wild type and Atp8a1 (-/-) mice were tested for hippocampal function using the water T-maze protocol. Results were from two sets of experiments, each performed with four mice in each of the two groups (Wild type and Atp8a1-/-). No dramatic sex difference was observed. Mice consistently committing two or less errors on two consecutive days were considered to have reached the criterion. *For both males and females Atp8a1 (-/-) vs. wild type $p < 0.014$. (V. Punia, P. Banerjee, unpublished data)

CHAPTER 4

DISCUSSION

Apoptosis or programmed cell death is an important event that occurs throughout the life span of an organism. During development, apoptosis is as essential as mitosis. For example, during the formation of fingers and toes of a fetus, removal of the tissue between them by apoptosis is needed. Also, the nervous system produces excess neurons, and only those neurons that are capable of forming proper synapses survive. The rest are eliminated by apoptosis. In homeostasis, apoptosis helps maintain a constant number of cells constant by balancing with mitosis.

Apoptosis is a clean process that eliminates unwanted cells avoiding the inflammatory problems of necrosis. Thus, it is the perfect process that can be used for eliminating cancer cells. Chemotherapy has been shown to function through the apoptotic pathway (Fisher 1994). There has been progress in understanding the events underlying drug-induced apoptosis. Several researchers have shown the involvement of caspases, especially caspase-8 and 9 (Sun 1999, Budihardjo 1999, Ferreira 2000). Chemotherapy is very effective in eliminating cancer cells, but it also adversely affects normal cells. In our quest to target brain cancer cells specifically without affecting normal cells, we first studied the current literature to understand how our immune system (phagocytes) differentiates between apoptotic and normal cells.

The well-known characteristic of the apoptotic cells is the presence of PS in the outer leaflet of the plasma membrane. In normal cells, PS remains in the inner leaflet and this asymmetric distribution of PS is maintained by plasma membrane

aminophospholipid translocases (APLTs), also known as flippases. The pathway by which PS is externalized during apoptosis is still unknown. A group of researchers have shown that cytochrome c released from the mitochondria oxidizes PS (present in the inner leaflet). They speculate that oxidized PS affects its recognition by APLTs, thus resulting in an inhibition of its activity. Consequently, PS remains in the outer leaflet of the plasma membrane where it gets recognized by PS receptor-bearing phagocytes (Kagan 2000, Tyurina 2000) (Figure 17).

The role of plasma membrane APLTs in maintaining PS asymmetry in the plasma membrane is crucial and inhibition of PM-APLTs could lead to PS exposure and phagocytosis of a cell. This is why we have tried to identify the protein or proteins responsible for the plasma membrane APLT activity in neuronal cells. Identification of this protein will help in our quest to target brain cancer cells. Our approach is to inhibit the APLT activity in brain cancer cells specifically, thus leading to their removal by the clean process phagocytosis.

As mentioned in the introduction, a well-known candidate for the plasma membrane APLT has been Atp8a1, which belongs to the Type IV subfamily of P-type ATPases. Atp8a1was purified (Moriyama 1988), and its cDNA was cloned (Tang 1996) from bovine chromaffin granules. Drs2, the Atp8a1 yeast homolog, is the founding member of the Type-IV subfamily of P-type ATPases, whereas the other members are putative APLTs (Ripmaster 1993, Tang 1996). Studies showed that a yeast strain (Δ*drs2*) lacking the Drs2 protein was unable to internalize NBD-PS (Tang 1996). Also, recently Darland-Ransom *et al* (Darland-Ransom 2008a) showed that the Atp8a1 C. *elegans* homolog (TAT-1) maintains PS in the inner leaflet of plasma membrane. However, there

is still controversy regarding the identification of the plasma membrane APLT and whether Atp8a1 functions in the plasma membrane or in intracellular organelles. For example, Graham's laboratory showed that Drs2p was localized to the yeast Golgi network rather than in the plasma membrane (Chen 1999, Devaux 2006). Also, recently *in vitro* analysis of the purified protein showed that Atp8a1 was similar to, but not the same as, the plasma membrane APLT (Paterson 2006). Finally, Züllig and coworkers reported that RNAi-mediated suppression of TAT-1 causes stimulation (rather than inhibition) of plasma membrane APLT activity, but, as stated above, Darland-Ransom and coworkers showed just the opposite effect.

Up to date there has been no report involving Atp8a1 as the plasma membrane APLT of neuronal or neurotumor cells. Here, we demonstrate that Atp8a1 is the plasma membrane APLT of the neuroblastoma cell line N18.

Interestingly, Atp8a1 APLT activity appears to be cell-type specific. In our studies, we tested two cell lines: a mouse neuroblastoma cell line (N18) and a hippocampal derived cell line (HN2). By searching through literature and analyzing different protocols, we put together a modified plasma membrane APLT assay. In this assay, as described in materials and methods, we are able to record changes in plasma membrane APLT activity by measuring the increase or decrease in fluorescence of NBD-PS present in the inner leaflet of the plasma membrane. The plasma membrane APLT activity is initiated at 28 °C (at which no endocytosis occurs). In Figure 8, we are able to visualize the internalization of NBD-PS to the inner leaflet of the plasma membrane as the incubation at 28 °C proceeds up to 10 min. The ability to measure only NBD-PS in the inner leaflet of the plasma membrane in this assay is made possible by the addition of

sodium dithionite after incubation at 28 °C. Sodium dithionite removes fluorescence from the outer leaflet (untranslocated NBD-PS) by reducing NBD-PS to ABD-PS (a non-fluorescent phospholipid) (Figure 7).

In our first set of experiments, we analyzed the effect of transient overexpression of Atp8a1 in the PM-APLT of the two cell lines (N18 and HN2) through a time-course APLT assay. These two cell lines were used because, as stated above, we wanted to identify the plasma membrane APLT of neuronal (differentiated HN2) and neurotumor (N18) cells. The results (Figure 9) obtained from these experiments showed that overexpression of Atp8a1 in N18 cells cause an increase in the plasma membrane APLT activity. However, this was not the case for the HN2 cells. Overexpression of Atp8a1 in differentiated HN2 caused a decrease in the plasma APLT. This led us to conclude that Atp8a1 was the plasma membrane APLT in N18 cells and thus hypothesizing that Atp8a1 could be the plasma membrane APLT of neurotumor cells and/or fast dividing cells.

To further support our results that Atp8a1 was the plasma membrane APLT of the N18 cells, we turned to enzyme kinetics. The kinetic parameters, Km and Vmax, helps in determining if the overexpressed enzyme is identical to the endogenous enzyme catalyzing a specific reaction. If Atp8a1 were indeed the plasma membrane APLT enzyme in N18 cells, then overexpression of this molecule would cause an increase in the Vmax value due to an increase in the number of the endogenous APLT molecules catalyzing the translocation of NBD-PS. Also, if Atp8a1 is identical to the endogenous PM-APLT, its overexpression or suppression should not change the Km value of PM-APLT. Thus, in our next experiments, we performed substrate concentration-dependant

APLT assays (as described in materials and methods). Km and Vmax values were calculated by graphing a Lineweaver-Burk plot. As expected and confirming our hypothesis, transient overexpression of Atp8a1 in N18 cells cause an increase in the Vmax value without affecting the Km value of the plasma membrane APLT activity (Figure 10 and table 2).

If overexpression of Atp8a1 causes an increase in the plasma membrane APLT activity of N18 cells as evidenced by an increase in Vmax, then suppression of Atp8a1 activity should lead to a decrease in the plasma membrane APLT activity and a decrease in the Vmax value. As expected, this was what we observed in the following experiments.

To suppress the activity of Atp8a1, we created phosphorylation-site mutants. In these mutants, the ability to hydrolyze ATP and translocate PS is hampered by a mutation in the aspartic acid residue of the P-type signature sequence. We believe that these phosphorylation-site mutants could be acting as possible dominant negative mutants, suppressing the activity of the wild-type Atp8a1. When we expressed the Atp8a1 phosphorylation-site mutants and measured the Km and Vmax values, we observed, as expected, a decrease in the Vmax value but no significant change in the Km value (Figure 11 and table 3). The concept of dominant negative mutations as a tool to study the function of specific genes was first introduced by Herskowitz in 1987 (Herskowitz 1987). Dominant negative mutants are capable of competing with the wild-type enzyme for its substrate. They can efficiently inhibit any functional consequence of the wild type enzyme if, and only if the enzymatic reaction is limited by the concentration of a protein that critically regulates the processing or activation of the enzyme. We postulate that the

limiting protein for which our Atp8a1 phosphorylation-site mutants compete with the wild-type Atp8a1is a chaperone-like protein such as CDC50. Studies have shown that the interaction between CDC50 and the Atp8a1 homolog, Atp8b1, is required for the release of this Type IV P-type ATPase from the endoplasmic reticulum (ER) and targeting to the plasma membrane (Paulusma 2008). CDC50 is a glycosylated protein (of approximately 60 kDa) and its importance in targeting Type IV P-type ATPases to the plasma membrane was first shown in yeast by Saito *et al* (Saito 2004). A mammalian homolog of CDC50 could be the chaperone binding to the Atp8a1 phosphorylation-site mutants, which could prevent the targeting of the wild-type Atp8a1 to the plasma membrane, and thereby inhibiting Atp8a1-catalyzed translocation of phosphatidylserine to the inner leaflet of the plasma membrane.

If indeed Atp8a1 is the plasma membrane APLT in N18 cells, then suppression of Atp8a1 by overexpression of the Atp8a1 phosphorylation-site mutants should lead to PS externalization. This is exactly what we observed when we measured PS externalization through the annexin V staining assay. Only cells with externalized PS will stain with annexin V, which was tagged with Alexa fluor 488. Expression of the two Atp8a1 mutants (Atp8a1-D409K and Atp8a1-D409E) caused an increase in annexin V staining in the N18 cells (Figure 12).

The suppression of Atp8a1 activity observed through the substrate-dependent PM-APLT assays and the annexin V staining assays was not 100%. This could be due to transient expression, which is at the most 80% efficient. However, another possibility could be that Atp8a1 is not be the only protein responsible for the plasma membrane APLT activity in N18 cells. To address this question, we decided to overexpress another

Type IV P-type ATPase, Atp8a2. We chose Atp8a2 because it is the closest paralog of Atp8a1. When we transiently overexpressed Atp8a2 in N18 cells, the plasma membrane APLT activity decreased. Results showed a decrease in both Vmax and Km values, signifying that Atp8a2 is not the plasma membrane APLT in these cells (displaying a different Km value) (Figure 13 and table 4). From this set of experiments we can also confirm that the increase in Vmax observed with the overexpression of Atp8a1 was not an artifact of transfection.

Together these results support our hypothesis that Atp8a1 is the plasma membrane APLT in N18 cells. We further hypothesized that Atp8a1 could be the plasma membrane APLT of fast-dividing neuroblasts. To test this postulate, we performed some preliminary experiments using an Atp8a1 (-/-) mouse strain.

It has become well accepted that neurogenesis (cell proliferation) occurs in the dentate gyrus (DG) of the hippocampus, a region important in memory and learning function. Thus, for our purpose of testing the hypothesis that Atp8a1 could be the plasma membrane APLT of fast dividing neuroblasts, we decided to focus our attention in the proliferating cells of the DG. To better understand the physiological importance of Atp8a1 and the consequence of its elimination in the fast diving neuroblasts of the DG, we used the Atp8a1 (-/-) mice, which were obtained by pairing Atp8a1 (+/-) from JAX lab. These mice did not have any reported, abnormal phenotypic characteristics. However, when we examined the asymmetric distribution of PS in the proliferating neuroblasts of the DG, we observed that many of those cells harbored exposed PS in the outer leaflet of the plasma membrane. We monitored PS externalization by annexin V

staining in dissociated cells from the DG and hippocampal culture slices of Atp8a1 (-/-) and wild type mice (Figure 14 and 15).

As mentioned previously, PS acts as a marker for phagocyte recognition when present in the outer leaflet of the plasma membrane. Thus, if Atp8a1 is the plasma membrane APLT of proliferating neuroblasts in the DG, then its absence in the Atp8a1 (-/-) mice leading to PS externalization, as observed in our results, should result in phagocytosis. Consequently, we could expect a loss of hippocampal neurons, which could contribute to impairment of learning and memory. To test this hypothesis, The Atp8a1 (-/-) mice were subjected to behavioral analysis by using the water T-maze. According to the results obtained, the Atp8a1 (-/-) mice appeared to suffer from delayed hippocampal learning as compared to the wild type mice (Figure 16). However, not all visual-based learning tests are hippocampal-dependant. To confirm that indeed elimination of Atp8a1 affects hippocampal functioning, a test such as the T-maze non-matching-to-place task will be used in our future studies. In this test, the spatial working memory is tested and impairments in the septo-hippocampal system are measured. Briefly, in the T-maze non-matching-to-place task, each trial consisted of a sample run and a choice run. On the sample run mice are forced either left or right by a wooden block to obtain a milk reward, according to a pseudorandom sequence in which equal numbers of left and right turns are done per session, and with no more than three consecutive turns in same direction. The block is then removed and mice are allowed a free choice of either arm. The time interval between the sample run and the choice run is about 15 sec. The mouse is rewarded for choosing the previously unvisited arm (i.e., for alternating) (Reisel *et al.* 2002).

Our studies presented here strong evidence indicating that Atp8a1 is the plasma membrane APLT of the neuroblastoma cell line N18, and most likely the plasma membrane APLT of the proliferating neuroblasts of the DG. Thus, this protein could play a serious role in the maintenance of normal hippocampal function. Our findings also open a new strategy for eliminating brain cancer cells by specifically suppressing Atp8a1 activity in neurotumor cells, which would cause their elimination through phagocytosis without affecting normal cells.

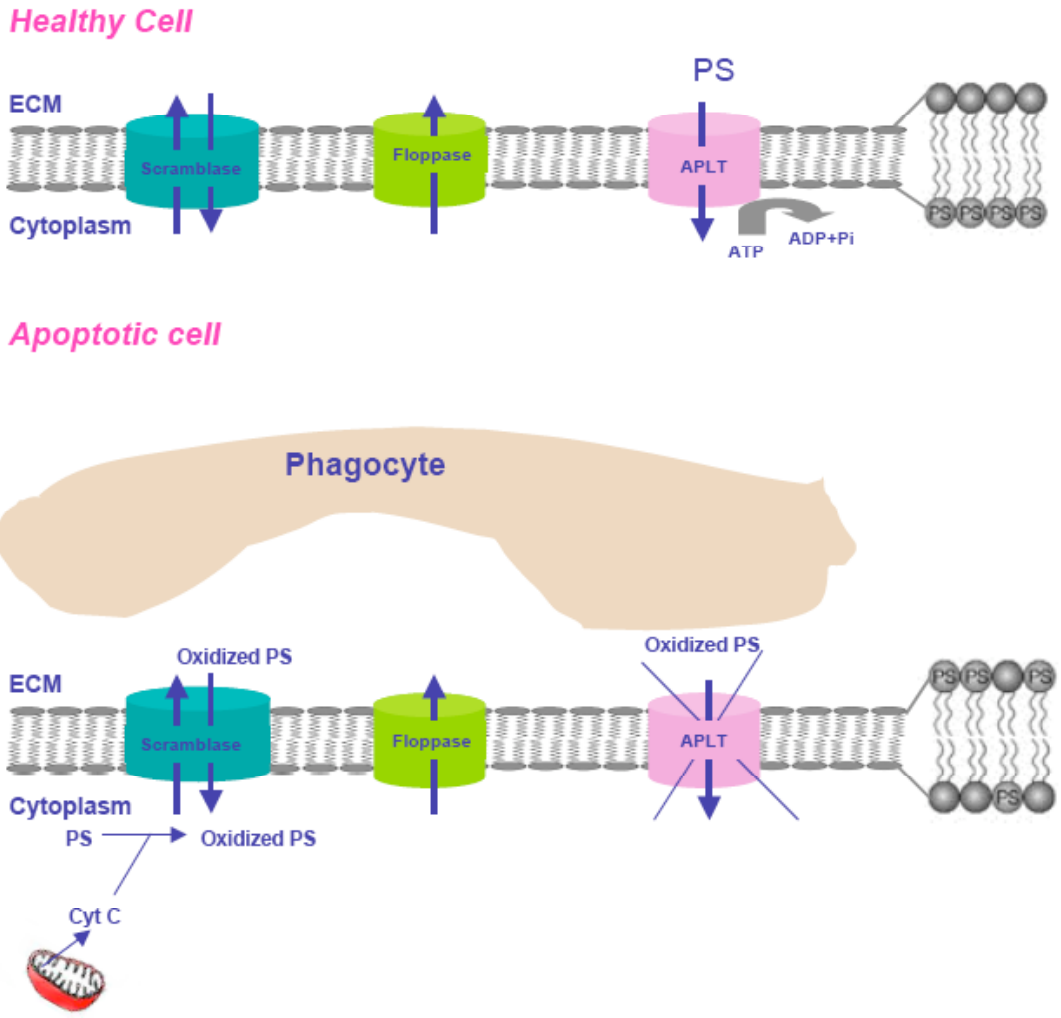

Figure 17: Proposed pathways by which PS is externalized during apoptosis.

References:

Anderson, H. A., Maylock, C. A., Williams, J. A., Paweletz, C. P., Shu, H., Shacter, E. (2003) Serum-derived protein S binds to phosphatidylserine and stimulates the phagocytosis of apoptotic cells. *Nat Immunol,* **4,** 87-91.

Arms, K., Camp, P. (1995) Biology (4th ed.). *New York: Harcourt Brace College Publishers*.

Ashkenazi, A. (2008) Directing cancer cells to self-destruct with pro-apoptotic receptor agonists. *Nat Rev Drug Discov,* **7,** 1001-1012.

Bao, Q., Shi, Y. (2007) Apoptosome: a platform for the activation of initiator caspases. *Cell Death Differ,* **14,** 56-65.

Beleznay, Z., Zachowski, A., Devaux, P., Navazo, M., Ott, P. (1993) ATP-dependent aminophospholipid translocation in erythrocyte vesicles: Stoichiometry of transport. *Biochemistry,* **32,** 3146-3152.

Bevers, E. M., Comfurius, P., Dekkers, D. W., Zwaal, R. F. (1999) Lipid translocation across the plasma membrane of mammalian cells. *Biochim Biophys Acta,* **1439,** 317-330.

Budihardjo, I., Oliver, H., Lutter, M., Luo, X., Wang, X. (1999) Biochemical pathways of caspase activation during apoptosis. *Annu Rev Cell Dev Biol,* **15,** 269-290.

Chen, C. Y., Ingram, M. F., Rosal, P. H., Graham, T. R. (1999) Role for Drs2p, a P-type ATPase and potential aminophospholipid translocase, in yeast late Golgi function. *J Cell Biol,* **147,** 1223-1236.

Chinnaiyan, A. M., O'Rourke, K., Tewari, M., Dixit, V. M. (1995) FADD, a novel death domain-containing protein, interacts with the death domain of Fas and initiates apoptosis. *Cell,* **81,** 505-512.

Connor, J., Pak,C.H., Zwaal,R.F.A., Schroit,A.J. (1992) Bidirectional Transbilayer Movement of Phospholipid Analogs in Human Red Blood Cells. *journal of Biological Chemistry,* **267,** 19412-19417.

Connor, J., Schroit, A. J. (1988) Transbilayer movement of phosphatidylserine in erythrocytes: inhibition of transport and preferential labeling of a 31,000-dalton protein by sulfhydryl reactive reagents. *Biochemistry,* **27,** 848-851.

Connor, J., Schroit, A. J. (1989) Transbilayer movement of phosphatidylserine in nonhuman erythrocytes: evidence that the aminophospholipid transporter is a ubiquitous membrane protein. *Biochemistry,* **28,** 9680-9685.

Coultas, L., Strasser, A. (2003) The role of the Bcl-2 protein family in cancer. *Semin Cancer Biol,* **13,** 115-123.

Daleke, D. L. (2003) Regulation of transbilayer plasma membrane phospholipid asymmetry. *Journal of Lipid Research,* **44,** 233-242.

Darland-Ransom, M., Wang, X., Sun, C. L., Mapes, J., Gengyo-Ando, K., Mitani, S., Xue, D. (2008a) Role of C. elegans TAT-1 protein in maintaining plasma membrane phosphatidylserine asymmetry. *Science,* **320,** 528-531.

Darland-Ransom, M., Wang, X., Sun, C.L., Mapes, J., Gengyo-Ando, K., Mitani, S., Xue, D. (2008b) Role od C. elegans TAT-1 Protein in Maintaining Plasma Membrane Phosphatidylserine Asymmetry. *Science,* **25,** 528-531.

Denayer, E., Ahmed, T., Brems, H., Van Woerden, G., Borgesius, N. Z., Callaerts-Vegh, Z., Yoshimura, A., Hartmann, D., Elgersma, Y., D'Hooge, R., Legius, E., Balschun, D. (2008) Spred1 is required for synaptic plasticity and hippocampus-dependent learning. *J Neurosci,* **28,** 14443-14449.

Devaux, P., López-Montero, I., Bryde, S. (2006) Proteins involved in lipid translocation in eukaryotic cells. *Chem Phys Lipids,* **141,** 119-132.

Devaux, P. F. (1992) Protein involvement in transmembrane lipid asymmetry. *Annual review of biophysics and biomolecular structure,* **21,** 417-439.

Ding, J., Wu, z., Crider, B., Ma, Y., Li, X., Slaughter, C., Gong, L. (2000) Identification and Functional Expression of Four Isoforms of ATPase II, the Putative Aminophospholipid Translocase. *the Journal of Biological Chemistry,* **275,** 23378-23386.

Fadok, V. A. (1999) Clearence: The Last and Often Forgatten Stage of Apoptosis. *Journal of Mammary Gland Biology and Neoplasia,* **4,** 203-211.

Fadok, V. A., Voelker, D. R., Campbell, P. A., Cohen, J. J., Bratton, D. L., Henson, P. M. (1992) Exposure of phosphatidylserine on the surface of apoptotic lymphocytes triggers specific recognition and removal by macrophages. *J Immunol,* **148,** 2207-2216.

Ferreira, C. G., Span, S. W., Peters, G. J., Kruyt, F. A., Giaccone, G. (2000) Chemotherapy triggers apoptosis in a caspase-8-dependent and mitochondria-controlled manner in the non-small cell lung cancer cell line NCI-H460. *Cancer Res,* **60,** 7133-7141.

Fisher, D. E. (1994) Apoptosis in cancer therapy: crossing the threshold. *Cell,* **78,** 539-542.

Halleck, M. S., Lawler JF, J. R., Blackshaw, S., Gao, L., Nagarajan, P., Hacker, C., Pyle, S., Newman, J. T., Nakanishi, Y., Ando, H., Weinstock, D., Williamson, P., Schlegel, R. A. (1999) Differential expression of putative transbilayer amphipath transporters. *Physiol Genomics,* **1,** 139-150.

Hart, S. P., Dransfield, I., Rossi, A. G. (2008) Phagocytosis of apoptotic cells. *Methods,* **44,** 280-285.

Henry-Mowatt, J., Dive, C., Martinou, J. C., James, D. (2004) Role of mitochondrial membrane permeabilization in apoptosis and cancer. *Oncogene,* **23,** 2850-2860.

Herskowitz, I. (1987) Functional inactivation of genes by dominant negative mutations. *Nature,* **329,** 219-222.

Ikeda, M., Kiahara, A., Igarashi, Y. (2006) Lipid asymmetry of the eukaryotic plasma membrane: Functions and related enzymes. *Biol. Pharm. Bull,* **29,** 1542-1546.

Kagan, V. E., Fabisiak, J. P., Shvedova, A. A., Tyurina, Y. Y., Tyurin, V. A., Schor, N. F., Kawai, K. (2000) Oxidative signaling pathway for externalization of plasma membrane phosphatidylserine during apoptosis. *FEBS Lett,* **477,** 1-7.

Kee, N., Teixeira, C. M., Wang, A. H., Frankland, P. W. (2007) Preferential incorporation of adult-generated granule cells into spatial memory networks in the dentate gyrus. *Nat Neurosci,* **10,** 355-362.

Kerr, J. F. R., Wyllie, A.H., Currie, A.R. (1972) Apoptosis: A Basic Biological Phenomenon With Wide-Ranging Implications in Tissue Kinetics. *Br.J.Cancer,* **26,** 239-257.

Kischkel, F. C., Hellbardt, S., Behrmann, I., Germer, M., Pawlita, M., Krammer, P. H., Peter, M. E. (1995) Cytotoxicity-dependent APO-1 (Fas/CD95)-associated proteins form a death-inducing signaling complex (DISC) with the receptor. *EMBO J,* **14,** 5579-5588.

Krysko, D., D'herde, K., Vandenabeele, P. (2006) Clearance of apoptotic and necrotic cells and its immunological consequences. *Apoptosis,* **11,** 1709-1726.

Kuchel, P. W., Ralston, G.B. (1988) Schaum's Outline of Theory and Problems of Biochemistry. Second ed. *New York: McGraw-Hill*.

Kuhlbrandt, W. (2004) Biology Structure and Mechanism of P-Type ATPases. *Nature reviews molecular cell biology,* **5,** 282-295.

Kühlbrandt, W. (2004) Biology, structure and mechanism of P-type ATPases. *Nat Rev Mol Cell Biol,* **5,** 282-295.

Lenoir, G., Williamson, P., Holthuis, J.C.M (2007) On the origin of lipid asymmetry: the flip side of ion transport. *Current Opinion in Chemical Biology,* **11,** 654-661.

Levano, K., Sobocki, T., Jayman, F., Debata, P. R., Sobocka, M. B. and Banerjee, P. (2009) A genetic strategy involving a glycosyltransferase promoter and a lipid translocating enzyme to eliminate cancer cells. *Glycoconj J.*

Maderna, P., Godson, C. (2003) Phagocytosis of apoptotic cells and the resolution of inflammation. *Biochim Biophys Acta,* **1639,** 141-151.

Martin, S. J., Reutelingsperger, C. P., McGahon, A. J., Rader, J. A., van Schie, R. C., LaFace, D. M., Green, D. R. (1995) Early redistribution of plasma membrane phosphatidylserine is a general feature of apoptosis regardless of the initiating stimulus: inhibition by overexpression of Bcl-2 and Abl. *J Exp Med,* **182,** 1545-1556.

McIntyre, J. C., Sleight,R.G. (1991) Fluorescence Assay for Phospholipid Membrane Asymmetry. *Biochemistry,* **20,** 11819-11827.

Mehta, M., Ahmed, Z., Fernando, S. S., Cano-Sanchez, P., Adayev, T., Ziemnicka, D., Wieraszko, A., Banerjee, P. (2007) Plasticity of 5-HT 1A receptor-mediated signaling during early postnatal brain development. *J Neurochem,* **101,** 918-928.

Moriyama, Y., Nelson, N. (1988) Purification and properties of a vanadate- and N-ethylmaleimide-sensitive ATPase from chromaffin granule membranes. *J Biol Chem,* **263,** 8521-8527.

Nagata, K., Ohashi, K., Nakano, T., Arita, H., Zong, C., Hanafusa, H., Mizuno, K. (1996) Identification of the product of growth arrest-specific gene 6 as a common ligand for Axl, Sky, and Mer receptor tyrosine kinases. *J Biol Chem,* **271,** 30022-30027.

Paterson, J. K., Renkema, K., Burden, L., Halleck, M. S., Schlegel, R. A., Williamson, P., and Daleke, D. L. (2006) Lipid Specific Activation of the Murine P_4-ATPase Atp8a1 (ATPase II). *Biochemistry,* **45,** 5367-5376.

Paulusma, C. C., Folmer, D. E., Ho-Mok, K. S., de Waart, D. R., Hilarius, P. M., Verhoeven, A. J., Oude Elferink, R. P. (2008) ATP8B1 requires an accessory protein for endoplasmic reticulum exit and plasma membrane lipid flippase activity. *Hepatology,* **47,** 268-278.

Paulusma, C. C., Oude Elfrerink, R.P. (2005) The type 4 subfamily of P-type ATPases, putative aminophospholipid translocases with a role in human disease. *Biochim Biophys Acta,* **1741,** 11-24.

Pomorski, T., Hrafnsdottir, S., Devaux, P.F., Van, G. (2001) Lipid distribution and transport across cellular membranes *Cell & Development Biology,* **12,** 139-148.

Ravichandran, K. S., Lorenz, U. (2007) Engulfment of apoptotic cells: signals for a good meal. *Nature reviews, immunology,* **7,** 964-974.

Reisel, D., Bannerman, D. M., Schmitt, W. B., Deacon, R. M., Flint, J., Borchardt, T., Seeburg, P. H. and Rawlins, J. N. (2002) Spatial memory dissociations in mice lacking GluR1. *Nat Neurosci,* **5,** 868-873.

Ripmaster, T. L., Vaughn, G. P., Woolford, J. L., Jr. (1993) DRS1 to DRS7, novel genes required for ribosome assembly and function in Saccharomyces cerevisiae. *Mol Cell Biol,* **13,** 7901-7912.

Saito, K., Fujimura-Kamada, K., Furuta, N., Kato, U., Umeda, M., Tanaka, K. (2004) Cdc50p, a protein required for polarized growth, associates with the Drs2p P-type ATPase implicated in phospholipid translocation in Saccharomyces cerevisiae. *Mol Biol Cell,* **15,** 3418-3432.

Seigneuret, M., Devaux, P. F. (1984) ATP-dependent asymmetric distribution of spin-labeled phospholipids in the erythrocyte membrane: relation to shape changes. *Proc Natl Acad Sci USA,* **81,** 3751-3755.

Sheppard, D. (1994) Dominant Negative Mutants: Tools for the Study of Protein Function In Vitro and In Vivo. *Am. J. Respir. Cell Mol. Biol.,* **11,** 1-6.

Sun, X. M., MacFarlane, M., Zhuang, J., Wolf, B. B., Green, D. R., Cohen, G. M. (1999) Distinct caspase cascades are initiated in receptor-mediated and chemical-induced apoptosis. *J Biol Chem,* **274,** 5053-5060.

Suzuki, H., Kamakura, M., Morii, M., Takeguchi, N. (1997) The phospholipid flippase activity of gastric vesicles. *J Biol Chem,* **272,** 10429-10434.

Tang, X., Halleck, M. S., Schlegel, R. A., Williamson, P. (1996) A subfamily of P-type ATPases with aminophospholipid transporting activity. *Science,* **272,** 1495-1497.

Teather, L. A., Magnusson, J. E., Chow, C. M., Wurtman, R. J. (2002) Environmental conditions influence hippocampus-dependent behaviours and brain levels of amyloid precursor protein in rats. *Eur J Neurosci,* **16,** 2405-2415.

Tilley, L., Cribier, S., Roelofsen, B., Op den Kamp, J. A., van Deenen, L. L. (1986) ATP-dependent translocation of amino phospholipids across the human erythrocyte membrane. *FEBS Lett,* **194,** 21-27.

Tyurina, Y. Y., Basova, L.V., Konduru, N.V.,Tyurin, V.A., Potapovich, A.I., Cai, P., Bayir, H.I., Stoyanovsky, D., Pitt, B.R., Shvedova, A.A., Fadeel, B., and Kagan V.E. (2007) Nitrosative Stress Inhibits the Aminophospholipid Translocase Resulting in Phosphatidylserine Externalization and Macrophage Engulfment. *journal of Biological Chemistry,* **282,** 8498-8509.

Tyurina, Y. Y., Shvedova, A. A., Kawai, K., Tyurin, V. A., Kommineni, C., Quinn, P. J., Schor, N. F., Fabisiak, J. P., Kagan, V. E. (2000) Phospholipid signaling in apoptosis: peroxidation and externalization of phosphatidylserine. *Toxicology,* **148,** 93-101.

Wang, J., Chun, H. J., Wong, W., Spencer, D. M., Lenardo, M. J. (2001) Caspase-10 is an initiator caspase in death receptor signaling. *Proc Natl Acad Sci U S A,* **98,** 13884-13888.

Zachowski, A., Favre, E., Cribier, S., Herve, P., Devaux, P. (1986) Outside-inside translocation of aminophospholipids in the human erythrocyte membrane is mediated by a specific enzyme. *Biochemistry,* **25,** 2585-2590.

Zullig, S., Neukomm, L.J., Jovanovic, M., Charette, S.J., Lyssenko, N.N., Halleck, M.S., Reutelingsperger, C.P.M., Schlegel, R.A., Hengartner, M.O. (2007) Aminophospholipid Translocase TAT-1 Promotes Phosphatidyserine Exposure during C. elegans Apoptosis. *Current Cell Biology,* **17,** 994-999.